Spectroscopic Foundations of Lasers: Spontaneous Emission Into a Resonator Mode

Marc Eichhorn and Markus Pollnau

(Invited Paper)

***Abstract*—We review the physics underlying the process of spontaneous emission, with a special focus on spontaneous emission into a resonator mode. We define the mode volume, verify the fundamental modal dimensions, present the spectral mode profile, the coherence time, the *Q*-factor, the Füchtbauer–Ladenburg equation, and the Purcell factor, and discuss their influence on different types of lasers. We obtain the relation between peak emission cross section, radiative lifetime, and emission linewidth. By interpreting spontaneous emission as stimulated emission driven by vacuum fluctuations, we derive the spontaneous-emission rate into a resonator mode and establish physical expressions for the fractions of spontaneous emission and total decay from the upper laser level into this mode. Furthermore, we discuss coupling of the atomic system with the coherent field inside a lasing resonator mode, resulting in the formation of a Mollow triplet, and demonstrate that it leads to a reduction of the spontaneous-emission rate into a coherently occupied resonator mode by a factor of 2.**

***Index Terms*—Lasers, optical resonators, laser modes, luminescence, spontaneous emission.**

I. Introduction

THE performance of lasers is often described by the laser rate equation, in which two processes that determine the number of coherent photons inside the laser resonator are considered, namely the stimulated-emission rate into the lasing resonator mode and the photon-decay rate out of this mode due to intrinsic resonator losses and outcoupling through the resonator mirrors. Frequently neglected in the laser rate equation is the photon source term that initializes laser operation, namely the spontaneous-emission rate into the lasing resonator mode. This approximation provides a simple and intuitive picture of how a continuous-wave (cw) laser operates: The laser threshold, which occurs at the point where the gain equals the losses, induces a sharp transition, above which the laser resonator fills with coherent photons in linear dependence on the pump rate of the upper laser level, whereas the inversion remains clamped to its threshold value. However, omission of the spontaneous-emission rate does not allow one to understand and quantify the coherence of a laser, its *Q*-factor and linewidth, how the laser operation is initialized, how the laser threshold depends on decay channels from the upper laser level i) at other transitions, ii) non-radiatively, and iii) into other optical modes, nor how threshold-less lasing can occur in micro-resonators.

In this paper, we review the physics underlying the process of spontaneous emission, with a special focus on spontaneous emission into a resonator mode. In a straight-forward manner we demonstrate that spontaneous emission can be interpreted as stimulated emission driven by the one vacuum photon per optical mode and polarization. We define the mode volume and present the relationship between spectral mode profile, coherence time, and *Q*-factor. Of importance for understanding spontaneous emission into a resonator mode is the derivation of the fundamental modal dimensions. We then obtain the relation between the radiative lifetime and the emission cross section, called the Füchtbauer–Ladenburg equation, introduce the Purcell factor to this equation, and discuss its influence on different types of lasers. We derive the relation between peak emission cross section, radiative lifetime, and emission linewidth and show that semiconductor and solid-state laser materials exhibit a similar product of radiative lifetime and peak emission cross section, because the atomic de-coherence of the excited state is on the same order of magnitude in both gain materials. We derive the spontaneous-emission rate into a resonator mode and establish physical expressions for the fractions of spontaneous emission and total decay from the upper laser level into this mode. Furthermore, we discuss coupling of the atomic system with a coherently occupied resonator mode, resulting in the splitting of the combined energy states into dressed states and occurrence of four spectrally separated emission lines, which at large coherent photon numbers form a Mollow triplet. For the first time, we show that this interaction reduces the spontaneous-emission rate into a coherently occupied resonator mode by a factor of two. We derive a novel expression for the effective spontaneous-emission cross section.

All phenomena are described in a coherent sequence and a self-consistent notation. The spectroscopic foundation laid in this paper will allow us to extend, in the same self-consistent notation, the laser rate equation by including the photon source term, thereby establishing a refined and more complete description of the cw laser [1].

II. Vacuum Photon and Spontaneous Emission

We interpret spontaneous emission of photons from upper to lower laser level as stimulated emission driven by vacuum

Manuscript received April 13, 2014; revised September 8, 2014; accepted September 23, 2014. Date of publication October 9, 2014; date of current version October 23, 2014. Both authors contributed equally to the work and therefore should be considered equivalent authors.

M. Eichhorn is with the French-German Research Institute of Saint-Louis ISL, F-68301 Saint Louis Cedex, France (e-mail: marc.eichhorn@isl.eu).

M. Pollnau is with the Department of Materials and Nano Physics, School of Information and Communication Technology, KTH–Royal Institute of Technology, 16440 Kista, Sweden (e-mail: m.pollnau@utwente.nl).

Color versions of one or more of the figures in this paper are available online at http://ieeexplore.ieee.org.

Digital Object Identifier 10.1109/JSTQE.2014.2361783

fluctuations. Since vacuum fluctuations create energy only within the related time uncertainty interval, they trigger only spontaneous emission [2]. Spontaneous absorption would lead to a long-lasting creation of energy, thereby violating the uncertainty principle [3], [4].

We assume that light at frequency ν propagates with speed $c = c_0/n_r(\nu)$, where c_0 is the speed of light in vacuum, in the active medium of refractive index $n_r(\nu)$, which homogeneously fills the mode volume V_{mode} of the resonator. With the wavenumber k and wavelength λ in the active medium,

$$\frac{k}{2\pi} = \frac{1}{\lambda} = \frac{\nu}{c} \tag{1}$$

when taking into account that in a 3-D Hohlraum resonator each mode extends over the round-trip length, i.e., forward (k) and backward ($-k$) propagating waves belong to the same mode, and the same mode volume V_{mode} is shared by two modes with orthogonal polarizations, in free space the mode density $M(\nu)$ per unit volume up to the frequency ν and the spectral mode density $\tilde{M}(\nu)$ are derived by the volume integral over the whole k-sphere:

$$\begin{aligned} M(\nu) &= 2\int_0^k \int_0^\pi \int_0^{2\pi} \frac{d^3k'}{(2\pi)^3} = 2\int_0^\nu \int_0^\pi \int_0^{2\pi} \frac{d^3\nu'}{c^3} \\ &= \frac{4\pi}{c^3}\int_0^\nu \int_0^\pi \nu'^2 \sin(\vartheta) d\vartheta d\nu' = \frac{8\pi\nu^3}{3c^3} \\ \Rightarrow \tilde{M}(\nu) &= \frac{dM(\nu)}{d\nu} = \frac{8\pi\nu^2}{c^3}. \end{aligned} \tag{2}$$

In this paper, all parameters that are defined per frequency interval, i.e., in units of the parameter divided by the frequency unit, are denoted by a tilde.

Exploiting Einstein's rate-equation description [2] of blackbody radiation, the radiative lifetime $\tau_{21,\mathrm{rad}}$ and rate constant or Einstein coefficient A_{21} of spontaneous emission are connected to the Einstein coefficient B_{21} of stimulated emission by

$$\frac{1}{\tau_{21,\mathrm{rad}}} = A_{21} = \frac{8\pi h\nu^3}{c^3} B_{21} = \tilde{M}(\nu) h\nu B_{21} \tag{3}$$

where h is Planck's constant. Interpreted as stimulated emission triggered by the vacuum spectral energy density $\tilde{u}_0(\nu)$ generated by the number φ_0 of vacuum photons of energy $h\nu$ per mode,

$$\tilde{u}_0(\nu) = \tilde{M}(\nu) h\nu \varphi_0, \tag{4}$$

the spontaneous-emission rate constant becomes

$$\frac{1}{\tau_{21,\mathrm{rad}}} = A_{21} = \tilde{u}_0(\nu) B_{21} = \tilde{M}(\nu) h\nu \varphi_0 B_{21}. \tag{5}$$

By comparison of (3) and (5) one obtains a fundamental result of quantum electrodynamics that

$$\varphi_0 = 1 \tag{6}$$

vacuum photon is present per mode as a result of vacuum fluctuations. In the present derivation, this result obtains from the information contained in Einstein's equation (3), see, e.g., Ref. [5]. The spectrum of blackbody radiation obeys Planck's equation [6], because (6) holds true.

III. Resonator Modes

In this section, we will define the mode volume of the Gaussian resonator mode, introduce its spectral mode profile, and derive the fundamental modal dimensions.

A. Mode Volume and Spatial Photon Density

For an optical resonator of geometrical length ℓ and the Gaussian TEM_{00} beam with beam waist w_0 as the resonator mode, the mode volume over which this resonator mode is distributed is

$$V_{\mathrm{mode}} = \ell \pi w_0^2. \tag{7}$$

V_{mode} is defined in the following way. The normalized spatial photon distribution function $\xi(r,z)$ describing the resonator mode is

$$\begin{aligned} \xi(r,z) &= \frac{1}{V_{\mathrm{norm}}} \frac{w_0^2}{w^2(z)} e^{-\frac{2r^2}{w^2(z)}} \\ \text{with } w(z) &= w_0\sqrt{1+\frac{z^2}{z_R^2}} \end{aligned} \tag{8}$$

where $w(z)$ is the beam radius at position z along the resonator axis, w_0 is the beam waist at position $z = 0$, $z_R = \pi w_0^2/\lambda$ is the Rayleigh range, and r and z are the radial and axial coordinate, respectively. The effective normalizing volume then is

$$V_{\mathrm{norm}} = \int_0^\ell \int_0^\infty \frac{w_0^2}{w^2(z)} e^{-\frac{2r^2}{w^2(z)}} 2\pi r dr dz = \frac{1}{2}\pi w_0^2 \ell = \frac{1}{2} V_{\mathrm{mode}}. \tag{9}$$

Thus, a photon density corresponding to φ photons in such a resonator mode is given by

$$\varphi\xi(r,z) = \frac{\varphi}{V_{\mathrm{norm}}} \frac{w_0^2}{w^2(z)} e^{-\frac{2r^2}{w^2(z)}} = \frac{2\varphi}{V_{\mathrm{mode}}} \frac{w_0^2}{w^2(z)} e^{-\frac{2r^2}{w^2(z)}}. \tag{10}$$

All energy densities, the population densities N_2 and N_1 of upper and lower laser level, respectively, as well as all rates considered in this work are photon-distribution averages which are defined, e.g., by calculating the average upper-level population density N_2 from its spatial distribution $N_2(r,z)$:

$$N_2 = \int_0^\ell \int_0^\infty N_2(r,z)\xi(r,z) 2\pi r dr dz. \tag{11}$$

Consequently, the average photon density of the photon distribution $\varphi\xi(r,z)$ obtains as

$$\begin{aligned} &\int_0^\ell \int_0^\infty \varphi\xi(r,z)\xi(r,z) 2\pi r dr dz = \int_0^\ell \int_0^\infty \varphi\xi^2(r,z) 2\pi r dr dz \\ &= \varphi \frac{1}{\ell^2\lambda} \arctan\left(\frac{\ell\lambda}{\pi w_0^2}\right) \approx \varphi \frac{1}{\pi w_0^2 \ell} = \frac{\varphi}{V_{\mathrm{mode}}}, \end{aligned} \tag{12}$$

showing explicitly that the average resonator photon density is the number of photons per mode volume V_{mode}. The approximation of the arctan is valid for short resonators with weakly diverging beams, i.e., in paraxial approximation, and an equality for an axially constant beam radius, e.g., in case of a guided mode in a waveguide that can be approximated by a collimated Gaussian distribution.

B. Spectral Mode Profile, Coherence Time, and Q-factor

A number $\varphi(t_0)$ of photons at frequency ν_0 that are present inside a resonator at the initial time t_0 decay out of the resonator with time t as a result of resonator losses which are quantified by the photon decay time τ_c (where the index c stands for "cavity", which means the resonator):

$$\varphi(t) = \varphi(t_0)e^{-t/\tau_c} \text{ for } t \geq t_0 = 0. \tag{13}$$

Fourier transformation of the amplitude of this exponential decay to frequency space and calculation of its absolute value squared,

$$\begin{aligned}\tilde{\gamma}_c(\nu) &= \frac{1}{\tau_c}\left|\frac{1}{\sqrt{\varphi(t_0)}}\int_{t_0}^{\infty}\sqrt{\varphi(t)}e^{-i2\pi(\nu-\nu_c)t}dt\right|^2 \\ &= \frac{1}{\tau_c}\left|\frac{2}{\pi}\frac{1}{i4(\nu-\nu_c)+(\pi\tau_c)^{-1}}\right|^2 \\ &= \frac{1}{\pi^2\tau_c}\frac{1}{4(\nu-\nu_c)^2+(2\pi\tau_c)^{-2}},\end{aligned} \tag{14}$$

provides the spectral intensity distribution of this emission as a function of frequency ν. It has a normalized Lorentzian spectral profile

$$\tilde{\gamma}_c(\nu) = \frac{2}{\pi}\frac{\Delta\nu_c}{4(\nu-\nu_c)^2+\Delta\nu_c^2} \quad \text{with} \int\tilde{\gamma}_c(\nu)d\nu = 1 \tag{15}$$

which is centered at frequency ν_c and of full-width-at-half-maximum (FWHM) linewidth

$$\Delta\nu_c = \frac{1}{2\pi\tau_c} = \frac{1}{\pi\tau_c^{\mathrm{coh}}}. \tag{16}$$

As illustrated in Fig. 1, the photon decay time τ_c is half the coherence time τ_c^{coh} of light emitted from the resonator, which, unlike an exponential decay, is defined over the interval from $t = -\infty$ to $t = \infty$ [7].

The quality of an optical resonator is expressed by its intrinsic Q-factor, originally introduced as the "coil dissipation constant" of a resonant electric circuit [8] and later generalized [9] as the energy stored in the resonator, E_{stored}, divided by the energy lost per oscillation cycle, E_{lost},

$$Q_c := 2\pi\frac{E_{\mathrm{stored}}(t)}{E_{\mathrm{lost}}(t)} = 2\pi\frac{\varphi(t)}{-\frac{1}{\nu_c}\frac{d}{dt}\varphi(t)} = 2\pi\nu_c\tau_c \tag{17}$$

where $E = h\nu_c\varphi$. Equations (17) and (16) relate the Q-factor and photon decay time to the linewidth, which can be measured by injecting continuous-wave (cw) light into the passive resonator, thus establishing a steady state in which the injected energy $E_{\mathrm{injected}} = E_{\mathrm{lost}} = E_{\mathrm{stored}}/(\nu_c\tau_c)$, and observing its spectral transmission

$$Q_c = 2\pi\left.\frac{E_{\mathrm{stored}}}{E_{\mathrm{injected}}}\right|_{\mathrm{cw}} = 2\pi\left.\frac{\varphi}{-\frac{1}{\nu_c}\frac{\delta\varphi}{\delta t}}\right|_{\mathrm{cw}} = 2\pi\nu_c\tau_c = \frac{\nu_c}{\Delta\nu_c}. \tag{18}$$

$\delta\varphi$ is the photon number lost during the time interval δt and replaced by injecting photons. The injection must take place via an existing loss channel of the resonator, e.g., one of the resonator mirrors, in order not to alter its Q-factor, and the injected signal must be optically isolated from its source to avoid feedback between the light-source resonator and the resonator under investigation.

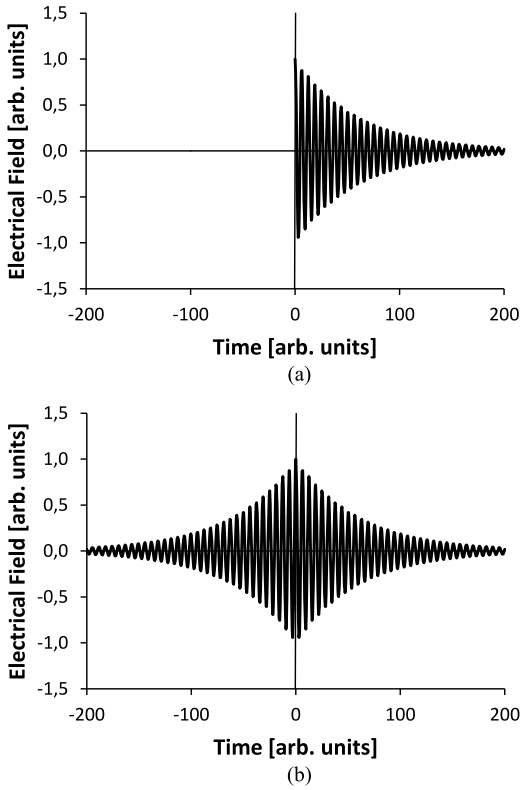

Fig. 1. Comparison of mathematical definitions of (a) photon decay time τ_c and (b) coherence time τ_c^{coh}.

Fourier transformation according to (14) and its Fourier back-transformation unambiguously transform the amplitudes of an exponential decay in the time domain and a Lorentzian line function in the frequency domain into each other, thereby relating the exponential decay time to the Lorentzian linewidth according to (16), i.e., the underlying physical process is independent of its description in frequency or time domain. Hence, the right-hand side of (18) serves as an equivalent definition of the Q-factor. In other words, the Q-factor of a passive resonator does not change with the way we feed light into it or the way we observe the outcoupled light. The Q-factor solely depends on the resonator losses.

Accordingly, in a passive Fabry–Pérot resonator [10] with a free spectral range of

$$\Delta\nu_{\mathrm{FSR}} = \frac{c}{2\ell} = \frac{1}{t_{\mathrm{RT}}} \tag{19}$$

where t_{RT} is the photon round-trip time in the resonator, each transverse-fundamental resonator mode with its longitudinal-mode index q, centered at frequency ν_q, where $\nu_0 = c/\lambda_0 = c/(2\ell)$ represents the lowest frequency, has an individual photon

decay time of $\tau_q(\nu_q)$ given by

$$\frac{1}{\tau_q(\nu_q)} = -\frac{c}{2\ell}\ln\left\{\left[1-L_{\mathrm{RT}}(\nu_q)\right]\left[1-T_{\mathrm{out}}(\nu_q)\right]\right\}, \quad (20)$$

where L_{RT} and T_{out} quantify the intrinsic round-trip losses and the out-coupling losses at the frequency ν_q, respectively. τ_q results in a Q-factor of Q_q according to (17) or (18), a linewidth of $\Delta\nu_q$ according to (16), and a finesse of

$$\mathscr{F}(\nu_q) = \frac{\Delta\nu_{\mathrm{FSR}}}{\Delta\nu_q} = \frac{\Delta\nu_{\mathrm{FSR}}}{\nu_q}Q_q = \frac{\lambda_q}{2\ell}Q_q = \frac{Q_q}{q+1}. \quad (21)$$

Each mode exhibits a normalized Lorentzian spectral profile equivalent to (15),

$$\tilde{\gamma}_q(\nu) = \frac{2}{\pi}\frac{\Delta\nu_q}{4(\nu-\nu_q)^2+\Delta\nu_q^2}. \quad (22)$$

The sum over all longitudinal modes results in a spectral airy function [11], [12]. The non-averaged spectral mode density of a single resonator mode with longitudinal-mode index q is given by

$$\tilde{M}_q(\nu) = \frac{\tilde{\gamma}_q(\nu)}{V_{\mathrm{mode}}}. \quad (23)$$

In case the Lorentzian line $\tilde{\gamma}_q(\nu)$ is narrow compared to the free spectral range of the resonator, the spectral mode density averaged over the free spectral range obtains as

$$\begin{aligned}\tilde{M}_{\mathrm{mode}}(\nu) &\approx \frac{1}{\Delta\nu_{\mathrm{FSR}}}\int_{\nu_q-\Delta\nu_{\mathrm{FSR}}/2}^{\nu_q+\Delta\nu_{\mathrm{FSR}}/2}\tilde{M}_q(\nu)d\nu \\ &= \frac{1}{\Delta\nu_{\mathrm{FSR}}}\int_{\nu_q-\Delta\nu_{\mathrm{FSR}}/2}^{\nu_q+\Delta\nu_{\mathrm{FSR}}/2}\frac{\tilde{\gamma}_q}{V_{\mathrm{mode}}}d\nu \\ &\approx \frac{1}{\Delta\nu_{\mathrm{FSR}}}\frac{1}{V_{\mathrm{mode}}}. \end{aligned} \quad (24)$$

In average, there exists one mode, hence also one vacuum photon φ_0, per polarization state and free-spectral range $\Delta\nu_{\mathrm{FSR}}$. Whereas $\tilde{M}_{\mathrm{mode}}(\nu)$ is only approximately equal to the finite integral in (24), which cuts off the wings of the Lorentzian profile $\tilde{\gamma}_q(\nu)$ of the single resonator mode of (23), the missing amount is exactly compensated by the wings of other resonator modes that reach into this free spectral range, hence the very left-hand and right-hand terms of (24) are equal to each other. Consideration of the solid angle of the resonator modes,

$$\begin{aligned}\Delta\Omega_{\mathrm{mode}} &= 2\times 2\pi\left[1-\cos(\theta)\right] \approx 4\pi\left[1-\left(1-\frac{1}{2}\theta^2\right)\right] \\ &= 2\pi\theta^2 = 2\frac{\lambda^2}{\pi w_0^2} = 2\frac{c^2}{\nu^2}\frac{1}{\pi w_0^2}, \end{aligned} \quad (25)$$

where θ is the divergence angle of the Gaussian beam and the factor of 2 takes both propagation directions into account, and executing the volume integral of (2) only over this solid angle,

$$\begin{aligned}M_{\mathrm{mode}} &= \int_0^{\nu}\int_{\Delta\Omega_{\mathrm{mode}}}\frac{d^3\nu'}{c^3} = \int_0^{\nu}\int_{\Delta\Omega_{\mathrm{mode}}}\frac{\nu'^2 d\Omega d\nu'}{c^3} \\ &= \int_0^{\nu}\frac{\nu'^2\Delta\Omega_{\mathrm{mode}}d\nu'}{c^3} = 2\frac{\nu}{c}\frac{1}{\pi w_0^2}, \end{aligned} \quad (26)$$

results in the same spectral mode density,

$$\tilde{M}_{\mathrm{mode}}(\nu) = \frac{dM_{\mathrm{mode}}}{d\nu} = \frac{2}{c}\frac{1}{\pi w_0^2} = \frac{2\ell}{c}\frac{1}{\pi w_0^2\ell} = \frac{1}{\Delta\nu_{\mathrm{FSR}}}\frac{1}{V_{\mathrm{mode}}}, \quad (27)$$

thereby proving that in (24) the very left-hand and right-hand terms are indeed equal.

C. Fundamental Modal Dimensions

When taking into account that in a 1-D linear resonator of length ℓ each mode extends over the round-trip length 2ℓ, i.e., forward (k) and backward ($-k$) propagating waves belong to the same mode, and the same mode volume is shared by two modes with orthogonal polarizations, the 1-D mode density $M^{1\mathrm{D}}(\nu)$ per unit length up to a frequency ν and the 1-D spectral mode density $\tilde{M}^{1\mathrm{D}}(\nu)$ along the resonator direction are given by

$$\begin{aligned}M^{1\mathrm{D}}(\nu) &= 2\int_{-k}^{k}\frac{dk'}{2\pi} = 2\int_0^{\nu}\frac{2d\nu'}{c} = \frac{4\nu}{c} \\ \Rightarrow \tilde{M}^{1\mathrm{D}}(\nu) &= \frac{dM^{1\mathrm{D}}(\nu)}{d\nu} = \frac{4}{c} = \frac{2}{\Delta\nu_{\mathrm{FSR}}}\frac{1}{\ell}. \end{aligned} \quad (28)$$

Although the volume integral in (2) ranges only from 0 to k, the integrated sphere includes negative and positive k values in all three dimensions. To cover the equivalent k-space, the 1-D integral in (28) must range from $-k$ to k. By inserting (19) into the right-hand side of (28), we find that two modes with orthogonal polarizations exist per free spectral range of the resonator of length ℓ, in agreement with (24). When considering the frequency range up to a maximum frequency ν, for transverse-fundamental-mode operation the 3-D spectral mode density inside the resonator amounts to

$$\frac{\tilde{M}^{1\mathrm{D}}(\nu)}{\pi w_M^2} = \frac{4}{c}\frac{1}{\pi w_M^2} = \frac{2}{\Delta\nu_{\mathrm{FSR}}}\frac{1}{\ell}\frac{1}{\pi w_M^2} = \tilde{M}(\nu) = \frac{8\pi\nu^2}{c^3}, \quad (29)$$

allowing us to determine the fundamental modal area πw_M^2 and radius w_M that are, in average, occupied by two resonator modes with orthogonal polarizations:

$$\pi w_M^2 = \frac{\tilde{M}^{1\mathrm{D}}(\nu)}{\tilde{M}(\nu)} = \frac{c^2}{2\pi\nu^2} = \frac{\lambda^2}{2\pi} \Rightarrow w_M = \frac{\lambda}{\sqrt{2}\pi}. \quad (30)$$

Inserting this result into (25) yields

$$\frac{\Delta\Omega_{\mathrm{mode}}}{4\pi} = \frac{\pi w_M^2}{\pi w_0^2}, \quad (31)$$

i.e., a mode confined to a beam waist w_0 that equals the fundamental modal radius w_M leads to divergence of the light propagation, in both directions, into the whole sphere, whereas a larger beam waist results in an accordingly smaller divergence.

The fundamental modal length that allows these two modes with orthogonal polarizations to exist inside the linear resonator equals one half sine cycle of light,

$$\ell_M = \frac{\lambda}{2}. \quad (32)$$

Physically interpreted, it encompasses one complete sine cycle over the round-trip length 2ℓ, leading to constructive interference of the wave with itself. As expected, with (19) the fundamental modal length results in a fundamental free spectral range of

$$\Delta\nu_{\mathrm{FSR},M} = \frac{c}{2\ell_M} = \nu. \tag{33}$$

The fundamental modal volume V_M that two linear-resonator modes with orthogonal polarizations would occupy if this volume did not spatially overlap with the volumes of any other modes then obtains with (30) and (32) as

$$V_M = \ell_M \pi w_M^2 = \frac{\lambda^3}{4\pi}. \tag{34}$$

This result for the fundamental modal volume is independent of the existence of a resonator, hence is the same as directly derived from the mode density in free space of (2) and the fundamental free spectral range of (33) by use of (1):

$$V_M = \frac{1}{\Delta\nu_{\mathrm{FSR},M}} \frac{2}{\tilde{M}(\nu)} = \frac{\lambda^3}{4\pi}. \tag{35}$$

If the volume V_{mode} is smaller than the fundamental modal volume V_M of (34), no resonator mode exists up to the maximum frequency ν. If V_{mode} equals $V_M(\nu)$, two orthogonal modes exist. If V_{mode} is larger than this limit, the number of modes and, hence, also the number of vacuum photons that, in average, share the volume V_{mode} of the lasing resonator mode increases stepwise to

$$\varphi_0(V_{\mathrm{mode}}) = 2\frac{V_{\mathrm{mode}}}{V_M(\nu)}. \tag{36}$$

These vacuum photons have largely different frequencies.

In a ring resonator, the round-trip length is identical to the geometrical length ℓ. Since forward and backward propagating modes then represent different modes, the total 1-D mode density of (28) remains equal to 4/*c*. The free spectral range of a ring resonator amounts to $\Delta\nu_{\mathrm{FSR}}(\mathrm{ring}) = c/\ell$, which is twice the value of (19). Nevertheless, the result of (30) remains unchanged, even for a unidirectional ring resonator, because both the 1-D mode density of that resonator and the equivalent free-space mode density, taking into account, e.g., only the positive *k*-direction, i.e., integrating only over a half sphere in (2), are both reduced by a factor of two. For the ring resonator, the fundamental modal length becomes equal to one wavelength, i.e., twice the value of (32). Therefore, the fundamental modal volume increases to twice that of a linear standing-wave resonator of (34).

IV. Transition Cross Sections and Emission Rates

The strengths of emission from the upper and absorption from the lower level of a transition can be described in terms of the effective emission and absorption cross sections $\sigma_e(\nu)$ and $\sigma_a(\nu)$, respectively, which are defined via the interaction of light at frequency ν with spectral intensity $\tilde{I}(\nu, z)$ propagating along the z direction and interacting with a gain medium:

$$\begin{aligned} \frac{d\tilde{I}(\nu,z)}{dz} &= \sigma_e(\nu) N_2(z) \tilde{I}(\nu,z) \\ \frac{d\tilde{I}(\nu,z)}{dz} &= -\sigma_a(\nu) N_1(z) \tilde{I}(\nu,z). \end{aligned} \tag{37}$$

In an active medium with crystal-field splitting of upper and lower electronic multiplets, $\sigma_e(\nu)/b_2 = \sigma_a(\nu)/b_1 = \sigma(\nu)$, where b_2 and b_1 are the Boltzmann factors of upper and lower crystal-field level of the specific transition at frequency ν, respectively, and $\sigma(\nu)$ is the atomic cross section of this transition (for simplicity, the degeneracies of the crystal-field levels are assumed to be equal).

A. Füchtbauer–Ladenburg Equation and Purcell Factor

Spontaneous emission that is interpreted as stimulated emission triggered by the vacuum spectral energy density $\tilde{u}_0(\nu)$, by use of (5), gives rise to a spectral fluorescence power $\tilde{P}_f(\nu)$ generated per unit volume *V* of

$$\frac{d\tilde{P}_f(\nu)}{dV} = -\frac{dN_2}{dt} h\nu \tilde{\rho}_f(\nu) = B_{21}\tilde{u}_0(\nu) N_2 h\nu \tilde{\rho}_f(\nu). \tag{38}$$

The spectral fluorescence distribution $\tilde{\rho}_f(\nu)$ is normalized to

$$\int \tilde{\rho}_f(\nu) d\nu = 1. \tag{39}$$

From the spectroscopic point of view, the same spectral fluorescence power $\tilde{P}_f(\nu)$ or spectral fluorescence intensity $\tilde{I}_f(\nu)$ can be regarded as a result of stimulated emission triggered by an equivalent plane-wave spectral vacuum photon intensity $\tilde{I}_0(\nu)$ generated per unit length z, penetrating the area A_{xy}, which, by use of (37), can be expressed as

$$\begin{aligned} \frac{d\tilde{P}_f(\nu)}{dV} &= \frac{\partial\tilde{P}_f(\nu)}{\partial A_{xy}\partial z} = \frac{d\tilde{I}_f(\nu)}{dz} \\ &= \sigma_e(\nu) N_2 \tilde{I}_0(\nu) = c\sigma_e(\nu) N_2 \tilde{u}_0(\nu). \end{aligned} \tag{40}$$

Equality of (38) and (40) yields

$$\sigma_e(\nu) = \frac{h\nu}{c} B_{21} \tilde{\rho}_f(\nu). \tag{41}$$

With (3), the emission cross section obtains as

$$\sigma_e(\nu) = \frac{1}{c} \frac{1}{\tau_{21,\mathrm{rad}}} \frac{1}{\tilde{M}(\nu)} \tilde{\rho}_f(\nu). \tag{42}$$

Exploiting (39) and (2) results in the Füchtbauer–Ladenburg equation in free space, which relates the effective emission cross section $\sigma_e(\nu)$ to the radiative lifetime $\tau_{21,\mathrm{rad}}$:

$$\frac{1}{\tau_{21,\mathrm{rad}}} = A_{21} = \int c\sigma_e(\nu)\tilde{M}(\nu) d\nu = \frac{8\pi}{c^2} \int \sigma_e(\nu)\nu^2 d\nu. \tag{43}$$

Accordingly, with (23), (2), and (22) the spontaneous-emission rate into a single resonator mode becomes

$$\frac{1}{\tau_{21,\mathrm{rad}}^{\mathrm{mode}}} = A_{21,\mathrm{rad}}^{\mathrm{mode}} = \int c\sigma_e(\nu)\tilde{M}_q(\nu)d\nu = \int c\sigma_e(\nu)\frac{\tilde{\gamma}_q(\nu)}{V_{\mathrm{mode}}}d\nu$$

$$= \int c\sigma_e(\nu)F_q(\nu)\tilde{M}(\nu)d\nu. \tag{44}$$

Therein,

$$F_q(\nu) = \frac{\tilde{M}_q(\nu)}{\tilde{M}(\nu)} = \frac{c^3}{8\pi\nu^2}\frac{\tilde{\gamma}_q(\nu)}{V_{\mathrm{mode}}}$$

$$= \frac{c^3}{4\pi^2\nu^2}\frac{1}{V_{\mathrm{mode}}}\frac{\Delta\nu_q}{4\left(\nu-\nu_q\right)^2+\Delta\nu_q^2} \tag{45}$$

quantifies the difference between the spontaneous-emission rate into a single resonator mode and that into free space.

In the limit of an emitter with a very narrow linewidth, $\Delta\nu_e \to 0$, if the resonator is tuned such that the center frequency ν_q of one of its modes matches the frequency ν_e of the peak cross section, the integral in (44) delivers a value different from zero only at frequencies $\nu \approx \nu_q = \nu_e$, equivalent to wavelengths $\lambda \approx \lambda_q = \lambda_e$ in the active medium, hence by use of (18) we can approximate (45) as

$$F_q(\nu) \overset{\substack{\Delta\nu_e\to 0\\ \nu=\nu_q=\nu_e}}{\approx} \frac{c^3}{4\pi^2\nu_q^2}\frac{1}{V_{\mathrm{mode}}}\frac{1}{\Delta\nu_q}$$

$$= \frac{c^3}{4\pi^2\nu_q^3}\frac{1}{V_{\mathrm{mode}}}Q_q = F_q(\nu_q)$$

$$\Rightarrow F_q(\lambda_q) = \frac{\lambda_q^3}{4\pi^2}\frac{1}{V_{\mathrm{mode}}}Q_q. \tag{46}$$

$F_q(\nu_q)$ and $F_q(\lambda_q)$ can be considered as a 1-D Purcell factor. Adding up this factor in all three dimensions results in the Purcell factor [13] that is defined for an emitter placed inside a 3-D hohlraum resonator:

$$3F_q(\lambda_q) = F_P(\lambda_q) = \frac{3\lambda_q^3}{4\pi^2}\frac{1}{V_{\mathrm{hohlraum}}}Q_q. \tag{47}$$

The radiative decay into the single resonator mode of (44) is then altered to

$$\frac{1}{\tau_{21,\mathrm{rad}}^{\mathrm{mode}}} = \int c\sigma_e(\nu)F_q(\nu)\tilde{M}(\nu)d\nu \overset{\substack{\Delta\nu_e\to 0\\ \nu=\nu_q=\nu_e}}{\approx}$$

$$F_q(\nu_q)\int c\sigma_e(\nu)\tilde{M}(\nu)d\nu = F_q(\nu_q)\frac{1}{\tau_{21,\mathrm{rad}}}. \tag{48}$$

Inserting (46), (45), (35), and (36) into (48) displays the underlying physics:

$$\frac{1}{\tau_{21,\mathrm{rad}}^{\mathrm{mode}}} \overset{\substack{\Delta\nu_e\to 0\\ \nu=\nu_q=\nu_e}}{\approx} \frac{\tilde{M}_q(\nu_q)}{\tilde{M}(\nu_q)}\frac{1}{\tau_{21,\mathrm{rad}}} = \frac{V_M}{2V_{\mathrm{mode}}}\frac{2}{\pi}Q_q\frac{1}{\tau_{21,\mathrm{rad}}}$$

$$= \frac{1}{\varphi_0(V_{\mathrm{mode}})}\frac{2}{\pi}Q_q\frac{1}{\tau_{21,\mathrm{rad}}}. \tag{49}$$

Compared to the spontaneous-emission rate $1/\tau_{21,\mathrm{rad}}$ into free space, the spontaneous-emission rate $1/\tau_{21,\mathrm{rad}}^{\mathrm{mode}}$ into the single resonator mode is, on the one hand, reduced by the factor $V_M/(2V_{\mathrm{mode}})$, because out of the number $\varphi_0(V_{\mathrm{mode}})$ of vacuum photons that in average occupy the mode volume V_{mode} only one triggers spontaneous emission into this mode. On the other hand, $1/\tau_{21,\mathrm{rad}}^{\mathrm{mode}}$ is enhanced by the factor Q_q, the resonant enhancement due to a high resonator quality, because the vacuum photon of this mode is better confined to the mode volume V_{mode} by this factor. Only when the latter factor is larger than the former, the spontaneous-emission rate into a single resonator mode exceeds that into free space.

In the other limit, if the effective emission cross-section $\sigma_e(\nu)$ varies insignificantly over the Lorentzian profile of the resonator mode, $\Delta\nu_e \gg \Delta\nu_q$, (45) and (44) can be approximated as

$$F_q(\nu_q) \overset{\Delta\nu_e >> \Delta\nu_q}{\approx} \frac{1}{\tilde{M}(\nu_q)}\frac{1}{\Delta\nu_{\mathrm{FSR}}}\frac{1}{V_{\mathrm{mode}}}$$

$$= \frac{c^3}{8\pi\nu_q^2}\frac{1}{\Delta\nu_{\mathrm{FSR}}}\frac{1}{V_{\mathrm{mode}}}, \tag{50}$$

$$\frac{1}{\tau_{21,\mathrm{rad}}^{\mathrm{mode}}} = \int c\sigma_e(\nu)\frac{\tilde{\gamma}_q(\nu)}{V_{\mathrm{mode}}}d\nu$$

$$\overset{\Delta\nu_e >> \Delta\nu_q}{\approx} \frac{c\sigma_e(\nu_q)}{V_{\mathrm{mode}}}\int\tilde{\gamma}_q(\nu)d\nu = \frac{c\sigma_e(\nu_q)}{V_{\mathrm{mode}}}. \tag{51}$$

For certain lasers with narrow spectral luminescence linewidth, $\Delta\nu_e \ll \Delta\nu_q$, e.g., far-infrared and sub-millimeter-wave lasers [14], as well as for solid-state and semiconductor lasers with resonator lengths that are not significantly longer than the laser wavelength, $\ell \approx \lambda_e$, leading to a large free spectral range in (19), a short photon decay time τ_q in (20), and an accordingly broad linewidth $\Delta\nu_q$ that can be on the order of $\Delta\nu_e$, see Fig. 2 (a), the integral in (44) must be considered, and experimentally the resonator length must be adjusted, such that ν_q equals the peak emission frequency ν_e, to ensure a large spectral overlap between the two profiles $\sigma_e(\nu)$ and $\tilde{\gamma}_L(\nu)$ of the lasing resonator mode [15].

In bulk lasers with resonator lengths that are long compared to the emission wavelength, $\ell \gg \lambda_e$, one finds an accordingly small free spectral range in (19), a long photon decay time τ_q in (20), and a narrow linewidth $\Delta\nu_q$. In, e.g., rare-earth-ion-doped near-infrared or visible solid-state lasers, phonon perturbation of the excited-state wave function, resulting in a virtual decay, as well as phononic re-distribution within the crystal-field multiplet, resulting in a real decay and re-population among the individual crystal-field levels, lead to atomic de-coherence with an atomic coherence time $\tau_{\mathrm{atom}}^{\mathrm{coh}}$. This decay occurs with a lifetime $\tau_{\mathrm{atom}} = 1/2\,\tau_{\mathrm{atom}}^{\mathrm{coh}}$, on the time scale of a picosecond, thus usually being significantly faster than the effective decay time $\tau_{2,\mathrm{eff}}$ and the radiative lifetime $\tau_{21,\mathrm{rad}}$ of the excited state, as well as the photon decay time τ_q in bulk lasers,

$$\frac{1}{2}\tau_{\mathrm{atom}}^{\mathrm{coh}} = \tau_{\mathrm{atom}} \ll \tau_{2,\mathrm{eff}}, \tau_{21,\mathrm{rad}}, \tau_q$$

$$\Rightarrow \Delta\nu_e = \frac{1}{2\pi}\left(\frac{1}{\tau_{\mathrm{atom}}}+\frac{1}{\tau_{2,\mathrm{eff}}}\right) \approx \frac{1}{2\pi\tau_{\mathrm{atom}}} \gg \Delta\nu_q, \tag{52}$$

thereby forming a key linewidth broadening mechanism. Consequently, with (16), one obtains $\Delta\nu_e \gg \Delta\nu_q$ in (52), hence the transition cross sections $\sigma_e(\nu)$ and $\sigma_a(\nu)$ are broader than, and vary insignificantly over, the Lorentzian profile $\tilde{\gamma}_q(\nu)$

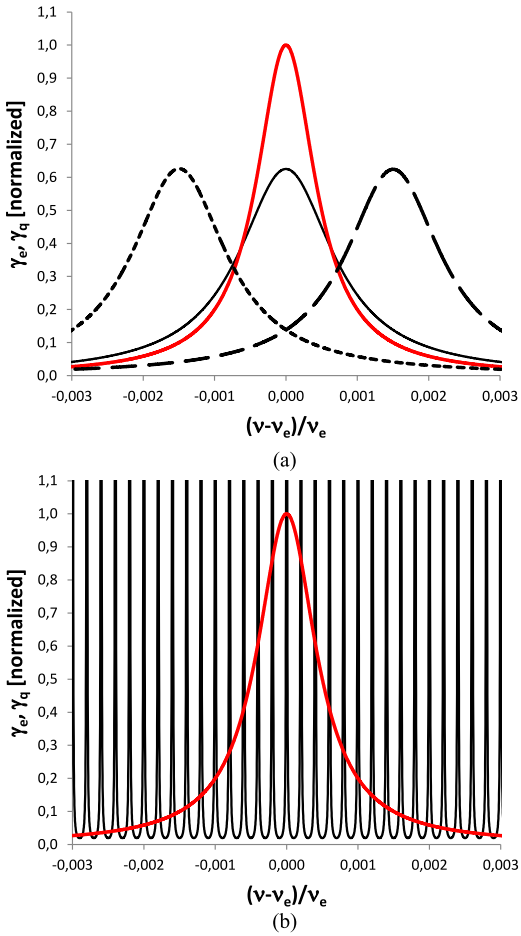

Fig. 2. Overlap of Lorentzian-shaped emission-line spectral profile $\tilde{\gamma}_e(\nu)$ (red) with Lorentzian-shaped resonator-mode spectral profiles $\tilde{\gamma}_q(\nu)$ (black), normalized to the peak of the emission-line spectral profile, for a resonator with $n_r = 1$, $\lambda_e = 1$ μm, $\Delta\lambda_e = 1$ nm, $T_{\rm out} = 0.01$, and $L_{\rm RT} = 0$, for resonator lengths of (a) $\ell = 1 \times \lambda_e/2$, showing the resonator mode with index $q = 0$ for ℓ (solid line) and detuning of ℓ by $\pm 0.15\%$ (dotted and dashed lines), and (b) $\ell = 5000 \times \lambda_e/2$, showing the 31 resonator modes with mode indices around $q = 4999$.

of the resonator mode, see Fig. 2 (b), such that (44) can be approximated by (51).

B. Relation Between Peak Emission Cross Section, Radiative Lifetime, and Emission Linewidth

For a single atomic emission line, centered at frequency ν_e, with a Lorentzian-shaped profile $\tilde{\gamma}_e(\nu)$ of linewidth $\Delta\nu_e$ given by (15), the emission cross section becomes

$$\sigma_e(\nu) = \sigma_e(\nu_e)\frac{\pi}{2}\Delta\nu_e\tilde{\gamma}_e(\nu) = \sigma_e(\nu_e)\frac{\Delta\nu_e^2}{4(\nu-\nu_e)^2+\Delta\nu_e^2}. \tag{53}$$

When assuming a narrow emission linewidth, $\Delta\nu_{e,\min} \ll \nu_e$, resulting in a large peak cross section $\sigma_{e,\max}(\nu_e)$, (43) yields

$$\frac{1}{\tau_{21,\rm rad}} \overset{\Delta\nu_e \ll \nu_e}{=} \frac{8\pi}{c^2}\int \sigma_{e,\max}(\nu_e)\frac{\pi}{2}\Delta\nu_{e,\min}\tilde{\gamma}_e(\nu)\nu_e^2 d\nu = \frac{4\pi^2\nu_e^2}{c^2}\sigma_{e,\max}(\nu_e)\Delta\nu_{e,\min}. \tag{54}$$

Exploiting (16) and (1),

$$\Delta\nu_{e,\min} = \frac{1}{2\pi\tau_{21,\rm rad}} = \frac{c}{\lambda_e^2}\Delta\lambda_{e,\min} \tag{55}$$

where $\Delta\lambda_{e,\min}$ is the minimum emission linewidth in wavelength units inside the active medium, one finds from (54) that the largest possible peak cross section, called the natural emission cross section, equals the fundamental modal area of (30):

$$\sigma_{e,\max}(\nu_e) = \frac{c^2}{4\pi^2\nu_e^2\tau_{21,\rm rad}}\frac{1}{\Delta\nu_{e,\min}} = \frac{c^2}{2\pi\nu_e^2} = \frac{\lambda_e^2}{2\pi} = \pi w_M^2. \tag{56}$$

With (53) and (56), the integral emission cross section Σ_e, i.e., the area underneath the spectral emission-cross-section curve, which is proportional to the product of peak emission cross section and emission linewidth, is solely determined by the radiative lifetime of spontaneous emission:

$$\Sigma_e = \int \sigma_e(\nu_e)\frac{\pi}{2}\Delta\nu_e\tilde{\gamma}_e(\nu)d\nu = \sigma_e(\nu_e)\frac{\pi}{2}\Delta\nu_e = \sigma_{e,\max}(\nu_e)\frac{\pi}{2}\Delta\nu_{e,\min} = \frac{c^2}{8\pi\nu_e^2\tau_{21,\rm rad}}. \tag{57}$$

Consequently, the product of peak emission cross section and radiative lifetime cannot exceed the value of

$$\sigma_e(\nu_e)\tau_{21,\rm rad} = \frac{c^2}{4\pi^2\nu_e^2}\frac{1}{\Delta\nu_e} = \frac{\lambda_e^4}{4\pi^2 c}\frac{1}{\Delta\lambda_e} \le \sigma_{e,\max}(\nu_e)\tau_{21,\rm rad} = \frac{c^2}{4\pi^2\nu_e^2}\frac{1}{\Delta\nu_{e,\min}} = \frac{\lambda_e^4}{4\pi^2 c}\frac{1}{\Delta\lambda_{e,\min}}. \tag{58}$$

Transitions within the 4*f* sub-shell of rare-earth ions are parity forbidden, leading to long radiative lifetimes on the order of $\tau_{21,\rm rad} \approx 10^{-3}$ s. Assuming a host material with a refractive index of $n_r = 2$, resulting in $c = c_0/n_r$, and an emission wavelength of $\lambda_e^{\rm vac} = 1$ μm emitted from the material, resulting in $\lambda_e = \lambda_e^{\rm vac}/n_r = 500$ nm, the emission linewidth expected from (55) would be as narrow as $\Delta\lambda_{e,\min} = \lambda_{e,\min}^{\rm vac}/n_r = 2.6 \times 10^{-19}$ m. From (56) one obtains a maximum peak emission cross section of $\sigma_{e,\max}(\lambda_e) = 4.0 \times 10^{-14}$ m^2. These values would satisfy (58). However, in rare-earth-ion-doped solid-state laser materials phonon perturbation of the excited-state wave function as well as phononic re-distribution within the crystal-field multiplet lead to atomic de-coherence with an atomic coherence time $\tau_{\rm atom}^{\rm coh}$ according to (52) on the time scale of $\tau_{\rm atom}^{\rm coh} \approx 10^{-12}$ s, orders-of-magnitude faster than $\tau_{21,\rm rad}$, resulting in the peak emission cross section being decreased and the emission linewidth $\Delta\lambda_e$ inside the active medium being increased by a factor of

$$f_\sigma = \frac{\Delta\nu_{e,\min}}{\Delta\nu_e} = \frac{\Delta\lambda_{e,\min}}{\Delta\lambda_e} = \frac{\sigma_e(\nu_e)}{\sigma_{e,\max}(\nu_e)} \overset{\tau_{\rm atom} \ll \tau_{21,\rm rad}}{\approx} \frac{\tau_{\rm atom}}{\tau_{21,\rm rad}} \tag{59}$$

on the order of $f_\sigma \approx 10^{-9}$, thereby leaving the integrated emission cross section of (57) and, thus, the radiative lifetime $\tau_{21,\rm rad}$

unchanged. The fast atomic de-coherence significantly broadens the emission linewidth to $\Delta\lambda_e \approx 0.5$ nm, equal to $\Delta\lambda_e^{\rm vac} \approx 1$ nm, and accordingly decreases the natural emission cross section of (57) to $\sigma_e(\nu_e) \approx 2 \times 10^{-23}$ m^2, thereby again satisfying (58). Thus, the significantly smaller experimental peak emission cross-sections observed in rare-earth-ion-doped host materials compared to the natural emission cross section obtained from (56) are not, as sometimes assumed, a direct consequence of the long lifetimes due to the parity rule, but of the ratio between these long lifetimes and the fast de-coherence of excited atomic states, as quantified by (59).

The allowed inter-band transitions in III–V semiconductor materials as well as the allowed transitions in laser dyes lead to significantly shorter radiative lifetimes on the order of $\tau_{21,\rm rad} \approx 10^{-7}$ s. Assuming that de-coherence of the excited states in these materials occurs at a similar time scale of $\tau_{\rm atom}^{\rm coh} \approx 10^{-12}$ s as in rare-earth-ion-doped materials, the linewidth-broadening and peak-decreasing factor f_σ is by a ratio of $10^{-7}/10^{-3} \approx 10^{-4}$ smaller in the semiconductor materials, leading to accordingly larger peak emission cross sections on the order of $\sigma_e \approx 10^{-20} - 10^{-19}$ m^2 in III–V semiconductor materials, compared to $\sigma_e \approx 10^{-24} - 10^{-23}$ m^2 in rare-earth-ion-doped materials [16]. In fact, the product of peak emission cross section $\sigma_e(\nu_e)$ and radiative lifetime $\tau_{21,\rm rad}$ in (58) is similar in these different classes of materials [16], because the de-coherence time is on the same order of magnitude. The situation is illustrated in a simplified manner in Fig. 3.

Taking the example of a host material, monoclinic potassium double tungstate, that is known for providing comparatively large emission cross sections to rare-earth ions such as Yb^{3+} [17], [18], its refractive index in the near-infrared spectral region is $n_r \approx 2$, resulting in $c \approx 1/2c_0$, and at the central emission line of $\lambda_e^{\rm vac} = 981$ nm, equal to $\lambda_e = 490$ nm in the active medium, the measured emission cross section is $\sigma_e(\lambda_e) \approx 1.5 \times 10^{-23}$ m^2, and the emission linewidth is $\lambda_e^{\rm vac} \approx 4.0$ nm, equal to $\Delta\lambda_e \approx 2.0$ nm in the active medium. The luminescence lifetime is $\tau_2 \approx 261$ μs [19]. However, the upper and lower state exhibit a crystal-field splitting into 3 and 4 crystal-field levels, respectively, resulting in 12 individual crystal-field transitions. Within each crystal-field multiplet, the population density is thermalized by fast phononic intra-multiplet transitions, resulting in a Boltzmann distribution. The radiative lifetime of spontaneous emission from upper to lower crystal-field multiplet reflects the decay on all 12 crystal-field transitions, whereas the area underneath the central line at 981 nm occupies only ~25% of the complete emission spectrum [19]. Hence, assuming that the decay from the upper crystal-field multiplet is entirely radiative, the spontaneous-emission rate on the central line corresponds to a radiative lifetime that is approximately four times the intrinsic luminescence lifetime, $\tau_{21,\rm rad} \approx 4\tau_2 \approx 1.044$ ms. Equivalent to (55), $\Delta\lambda_e \approx 2.0$ nm results in $\tau_{\rm atom} \approx 1.3 \times 10^{-13}$ s, thereby assuming that the measured emission linewidth is entirely due to atomic de-coherence and additional inhomogeneous linewidth-broadening mechanisms are negligible. Therefore, $f_\sigma = \tau_{\rm atom}/\tau_{21,\rm rad} \approx 1.2 \times 10^{-10}$. The decrease in peak emission cross section leads to $f_\sigma = \sigma_e(\lambda_e)/\sigma_{e,\max}(\lambda_e) = 1.5 \times 10^{-23}$ m^2/3.8×10^{-14} m^2 $= 3.9 \times 10^{-10}$, and the broadening of emission linewidth results in $f_\sigma = \Delta\lambda_{e,\min}/\Delta\lambda_e = 2.4 \times 10^{-19}$ m/2.0×10^{-9} m $= 8.2 \times 10^{-9}$. Consequently, the experimental values of $\sigma_e(\lambda_e) \approx 1.5 \times 10^{-23}$ m^2, $\tau_{21,\rm rad} \approx 1.044$ ms, and $\Delta\lambda_e \approx 2.0$ nm satisfy (58) only with an error of a factor of five, which may be owing partly to experimental inaccuracies when measuring these values, a spectral overlap of the central emission line with other nearby crystal-field transitions, additional inhomogeneous linewidth broadening, a certain amount of non-radiative decay from the upper crystal-field multiplet, which decreases the intrinsic luminescence lifetime from its radiative value to the measured value of $\tau_{2,\rm eff}$, and considering only one of the three directions of the optical indicatrix.

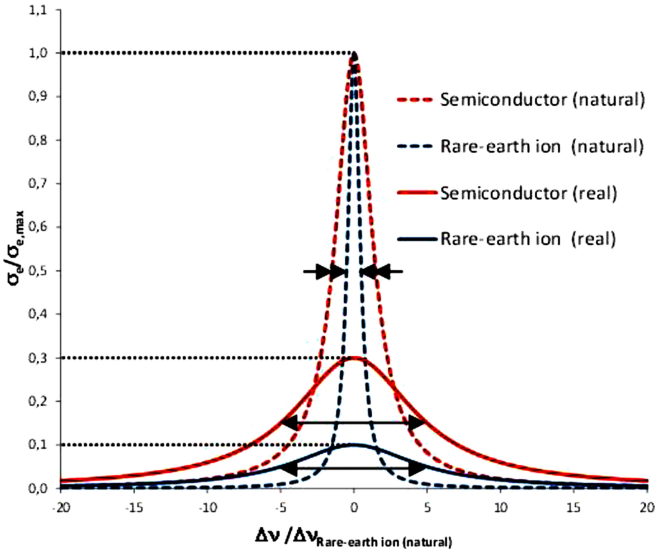

Fig. 3. Emission cross sections in a semiconductor and a rare-earth-ion-doped material, calibrated to the natural emission cross section, as a function of frequency detuning from the emission peak, calibrated to the FWHM linewidth of the natural emission line of the rare-earth ion. For the purpose of clarity of illustration in a single figure, it is assumed that the excited-state lifetime of the semiconductor is only three times (instead of orders-of-magnitude) shorter than that of the rare-earth ion, whereas the atomic de-coherence time is the same for both excited states and only 10 times (instead of orders-of-magnitude) shorter than the excited-state lifetime of the rare-earth ion. It results in $f_\sigma = 10$ for the rare-earth ion, $f_\sigma = 3.33$ for the semiconductor, and an experimentally observed (real) peak emission cross section which is 3 times larger for the semiconductor compared to the rare-earth ion. The arrows indicate the FWHM linewidths. The areas underneath the natural and experimentally observed (real) semiconductor emission lines are equal to each other. The same holds for the areas underneath the two rare-earth-ion emission lines.

V. Spontaneous Emission Into a Resonator Mode

In this section, we derive physical expressions for the fractions $\beta_{\rm mode}$ of spontaneous-emission rate and β of upper-state decay rate into a resonator mode, obtain a simple expression for the spontaneous-emission rate into this mode, and identify the time it takes for a photon to be spontaneously emitted into this mode.

A. The Fraction β_{mode} of Spontaneous-Emission Rate Into the Resonator Mode

In the presence of a resonator, luminescence can be emitted into the transverse-fundamental longitudinal resonator modes. With (44), the radiative lifetime describing this part of the emission is given by

$$\frac{1}{\tau_{21,\mathrm{rad}}^{tf-\mathrm{modes}}} = 2\sum_q \int c\sigma_e(\nu)\tilde{M}_q(\nu)d\nu = 2\sum_q \int c\sigma_e(\nu)\frac{\tilde{\gamma}_q(\nu)}{V_{\mathrm{mode}}}d\nu. \tag{60}$$

If the effective emission cross section $\sigma_e(\nu)$ varies insignificantly over the Lorentzian profile $\tilde{\gamma}_q(\nu)$ of each resonator mode, $\Delta\nu_e \gg \Delta\nu_q$, this part can be approximated by

$$\frac{1}{\tau_{21,\mathrm{rad}}^{tf-\mathrm{modes}}} \overset{\Delta\nu_e\gg\Delta\nu_q}{\approx} 2\sum_q \frac{c\sigma_e(\nu_q)}{V_{\mathrm{mode}}}\int\tilde{\gamma}_q(\nu)d\nu = 2\sum_q \frac{c\sigma_e(\nu_q)}{V_{\mathrm{mode}}}. \tag{61}$$

The mode density within the solid angle $\Delta\Omega$ of (25), which is occupied by the transverse-fundamental longitudinal resonator modes, is given by (27). Consequently, the radiative lifetime describing the emission of luminescence into this solid angle in free space would have amounted to

$$\frac{1}{\tau_{21,\mathrm{rad}}^{\Delta\Omega}} = 2\int c\sigma_e(\nu)\tilde{M}_{\mathrm{mode}}(\nu)d\nu = 2c\frac{1}{\Delta\nu_{\mathrm{FSR}}}\frac{1}{V_{\mathrm{mode}}}\int\sigma_e(\nu)d\nu. \tag{62}$$

If the effective emission cross section $\sigma_e(\nu)$ varies insignificantly over the Lorentzian profiles of many, and eventually all, resonator modes, $\Delta\nu_e \gg \Delta\nu_{\mathrm{FSR}} \gg \Delta\nu_q$, this lifetime can be approximated by

$$\frac{1}{\tau_{21,\mathrm{rad}}^{\Delta\Omega}} \overset{\Delta\nu_e\gg\Delta\nu_{\mathrm{FSR}}\gg\Delta\nu_q}{\approx} 2c\frac{1}{\Delta\nu_{\mathrm{FSR}}}\frac{1}{V_{\mathrm{mode}}}\sum_q\sigma_e(\nu_q)\Delta\nu_{\mathrm{FSR}} = 2\sum_q\frac{c\sigma_e(\nu_q)}{V_{\mathrm{mode}}} \overset{\Delta\nu_e\gg\Delta\nu_q}{\approx} \frac{1}{\tau_{21,\mathrm{rad}}^{tf-\mathrm{modes}}}. \tag{63}$$

If the resonator is of such a nature that it suppresses, by an appropriate photonic structure, emission into some of the external modes with a corresponding spectral mode density of $\tilde{M}_{\mathrm{suppr}}(\nu)$, which would otherwise have resulted in a radiative lifetime given by

$$\frac{1}{\tau_{21,\mathrm{rad}}^{\mathrm{suppr}}} = \int c\sigma_e(\nu)\tilde{M}_{\mathrm{suppr}}(\nu)d\nu, \tag{64}$$

for luminescence that is emitted into the 3-D space outside the solid angle $\Delta\Omega$ of the transverse-fundamental resonator modes only a spectral mode density of

$$\tilde{M}_{\mathrm{ext}}(\nu) = \tilde{M}(\nu) - \tilde{M}_{\mathrm{suppr}}(\nu) - 2\tilde{M}_{\mathrm{mode}}(\nu) \tag{65}$$

is available and, with (43), (64), and (62), this part yields a radiative lifetime of

$$\frac{1}{\tau_{21,\mathrm{rad}}^{\mathrm{ext}}} = \int c\sigma_e(\nu)\tilde{M}_{\mathrm{ext}}(\nu)d\nu = \frac{1}{\tau_{21,\mathrm{rad}}} - \frac{1}{\tau_{21,\mathrm{rad}}^{\mathrm{suppr}}} - \frac{1}{\tau_{21,\mathrm{rad}}^{\Delta\Omega}}. \tag{66}$$

Only under the condition $\Delta\nu_e \gg \Delta\nu_{\mathrm{FSR}} \gg \Delta\nu_q$, it can be approximated by

$$\frac{1}{\tau_{21,\mathrm{rad}}^{\mathrm{ext}}} \overset{\Delta\nu_e\gg\Delta\nu_{\mathrm{FSR}}\gg\Delta\nu_q}{\approx} \frac{1}{\tau_{21,\mathrm{rad}}} - \frac{1}{\tau_{21,\mathrm{rad}}^{\mathrm{suppr}}} - \frac{1}{\tau_{21,\mathrm{rad}}^{tf-\mathrm{modes}}}. \tag{67}$$

Thus, the radiative lifetime of an excited state inside the resonator is given by

$$\frac{1}{\tau_{21,\mathrm{rad}}^{\mathrm{res}}} = \frac{1}{\tau_{21,\mathrm{rad}}^{\mathrm{ext}}} + \frac{1}{\tau_{21,\mathrm{rad}}^{tf-\mathrm{modes}}} \overset{\Delta\nu_e\gg\Delta\nu_{\mathrm{FSR}}\gg\Delta\nu_q}{\approx} \frac{1}{\tau_{21,\mathrm{rad}}} - \frac{1}{\tau_{21,\mathrm{rad}}^{\mathrm{suppr}}} \overset{\tilde{M}_{\mathrm{suppr}}(\nu)=0}{=} \frac{1}{\tau_{21,\mathrm{rad}}}. \tag{68}$$

Hence, the radiative lifetime on the transition from upper to lower state of a gain medium inside the resonator is the same as the one of this medium in free space only if the emission spectrum is very broad compared to the free spectral range of the resonator, having itself narrow resonances, and emission into none of the external modes is suppressed.

Taking these considerations into account, the fraction of spontaneous emission from upper to lower state that is coupled into a specific mode and polarization of the resonator is correctly defined as

$$\beta_{\mathrm{mode}} := \frac{1\Big/\tau_{21,\mathrm{rad}}^{\mathrm{mode}}}{1\Big/\tau_{21,\mathrm{rad}}^{\mathrm{res}}} \le 1. \tag{69}$$

If all external resonator modes are suppressed and emission is possible only into the longitudinal, transverse-fundamental resonator modes, which are further restricted to one polarization, by use of (44) and (60) the fraction β_{mode} of the mode with longitudinal-mode index $m = \mathrm{Integer}(2\ell/\lambda - 1/2)$ that is closest to the peak of the spontaneous-emission line, (69) then becomes

$$\beta_{\mathrm{mode}} = 2\frac{1\Big/\tau_{21,\mathrm{rad}}^{\mathrm{mode}}}{1\Big/\tau_{21,\mathrm{rad}}^{tf-\mathrm{modes}}} = \frac{\int\sigma_e(\nu)\tilde{\gamma}_m(\nu)d\nu}{\sum_{q=0}^{\infty}\int\sigma_e(\nu)\tilde{\gamma}_q(\nu)d\nu} \le 1. \tag{70}$$

Assuming that the emission line is of Lorentzian shape, by inserting (53), the overlap integral of (44) takes the analytical form

$$\int c\sigma_e(\nu)\frac{\tilde{\gamma}_q(\nu)}{V_{\mathrm{mode}}}d\nu = \frac{c\sigma_e(\nu_e)}{V_{\mathrm{mode}}}\frac{\Delta\nu_e(\Delta\nu_q+\Delta\nu_e)}{4(\nu_e-\nu_q)^2+(\Delta\nu_q+\Delta\nu_e)^2}. \tag{71}$$

With (60), (71), (19), and (57) we obtain

$$\begin{aligned}\frac{1}{2}\frac{1}{\tau_{21,\mathrm{rad}}^{tf-\mathrm{modes}}} &= \sum_{q=0}^{\infty}\int c\sigma_e(\nu)\frac{\tilde{\gamma}_q(\nu)}{V_{\mathrm{mode}}}d\nu \\ &= \frac{c\sigma_e(\nu_e)}{\ell\pi w_0^2}\sum_{q=0}^{\infty}\frac{\Delta\nu_e(\Delta\nu_q+\Delta\nu_e)}{4(\nu_e-\nu_q)^2+(\Delta\nu_q+\Delta\nu_e)^2} \\ &= 2\Delta\nu_{\mathrm{FSR}}\frac{\sigma_e(\nu_e)}{\pi w_0^2}\sum_{q=0}^{\infty}\frac{\Delta\nu_e(\Delta\nu_q+\Delta\nu_e)}{4(\nu_e-\nu_q)^2+(\Delta\nu_q+\Delta\nu_e)^2} \\ &\overset{\ell\to\infty}{=} 2\frac{\sigma_e(\nu_e)}{\pi w_0^2}\lim_{\Delta\nu_{FSR}\to 0}\sum_{q=0}^{\infty}\frac{\Delta\nu_e(\Delta\nu_q+\Delta\nu_e)\Delta\nu_{\mathrm{FSR}}}{4(\nu_e-\nu_q)^2+(\Delta\nu_q+\Delta\nu_e)^2} \\ &= 2\frac{\sigma_e(\nu_e)}{\pi w_0^2}\int\frac{\Delta\nu_e^2}{4(\nu_e-\nu)^2+\Delta\nu_e^2}d\nu \\ &= 2\frac{\sigma_e(\nu_e)}{\pi w_0^2}\frac{\pi}{2}\Delta\nu_e = 2\frac{\Sigma_e}{\pi w_0^2}. \end{aligned} \tag{72}$$

It means that, for long resonator lengths, a very large number of longitudinal resonator modes overlapping with the spontaneous-emission line interrogate the integral emission cross section. The relative enhancement of spontaneous-emission rate at a specific resonator length ℓ with respect to the spontaneous-emission rate at $\ell\to\infty$ is then given by

$$\begin{aligned} f_\tau &= \frac{1}{2}\frac{1}{\tau_{21,\mathrm{rad}}^{tf-\mathrm{modes}}}\Bigg/\frac{2\Sigma_e}{\pi w_0^2} \\ &= \frac{c}{\ell\pi}\sum_{q=0}^{\infty}\frac{\Delta\nu_q+\Delta\nu_e}{4(\nu_e-\nu_q)^2+(\Delta\nu_q+\Delta\nu_e)^2}\overset{\ell\to\infty}{=}1. \end{aligned} \tag{73}$$

This situation is shown in Fig. 4. As can be seen in the upper row, a significant enhancement of spontaneous emission, the Purcell effect, occurs for short resonators when the resonator length is tuned such that a mode overlaps with the emission line, whereas a significant suppression of spontaneous emission occurs when the overlap of the emission line even with the nearest resonator mode is weak. For increasing resonator length ℓ the mode volume increases, thereby reducing the enhancement. For long resonators, in which many longitudinal modes overlap with the emission line, the enhancement converges to unity, i.e., the spontaneous-emission rate becomes independent of the resonator length and spectral tuning of the resonator is not necessary. For short resonators on the order of the emission wavelength, the fraction β_{mode} approaches unity when a resonator mode is tuned to the emission line. However, there are no sharp resonances, because β_{mode} represents the relative fraction of spontaneous emission into a single mode. At short resonator lengths, where only the nearest longitudinal resonator mode can significantly overlap with the emission line, detuning results in a reduction of the emission rate which, nevertheless, occurs significantly into this one mode only, hence β_{mode} remains large. Detuning of ℓ beyond $\lambda_e/4$ from the central wavelength of a mode increases β_{mode} again, because then the nearest mode is the next longitudinal mode. Detuning ℓ by exactly $\lambda_e/4$, providing equal overlap of the emission line with the two nearest modes of lower and higher frequency, results in a minimum value of β_{mode}, which is slightly lower than ½ due to the contributions of the second-nearest modes on either side. This behavior remains almost unchanged for a number of modes tuned across the emission line. For longer resonators, several modes overlap with the emission line and the luminescence decay occurs into these modes with comparable strength, thereby reducing the maximum obtainable β_{mode} for emission into a single mode and, hence, the contrast of the oscillations. For very long resonators, the oscillations in β_{mode} die out and β_{mode} decreases inversely proportional to the resonator length.

If the effective emission cross-section $\sigma_e(\nu)$ varies insignificantly over the Lorentzian profiles of many, and eventually all, resonator modes, $\Delta\nu_e > \Delta\nu_{\mathrm{FSR}} > \Delta\nu_q$, one can approximate (69) as

$$\beta_{\mathrm{mode}}\overset{\Delta\nu_e\gg\Delta\nu_{\mathrm{FSR}}\gg\Delta\nu_q}{\approx}\frac{c\sigma_e(\nu_q)\tau_{21,\mathrm{rad}}^{\mathrm{res}}}{V_{\mathrm{mode}}}\le 1. \tag{74}$$

Only when none of the external modes is suppressed, (74) can be further approximated to

$$\beta_{\mathrm{mode}}\overset{\tilde{M}_{\mathrm{suppr}}(\nu)=0}{\approx}\frac{c\sigma_e(\nu_q)\tau_{21,\mathrm{rad}}}{V_{\mathrm{mode}}}\le 1. \tag{75}$$

As we see from Fig. 4, if the mode volume is reduced to the fundamental modal dimensions, $V_{\mathrm{mode}}\to V_{\mathrm{M}}$, specifically $\ell=\ell_M$ or a reasonably small integer multiple of ℓ_M, the emission is restricted to one polarization, and all external modes are suppressed, $1/\tau_{21,\mathrm{rad}}^{\mathrm{suppr}}\to 1/\tau_{21,\mathrm{rad}}^{\mathrm{ext}}$, then in (74) $\tau_{21,\mathrm{rad}}^{\mathrm{res}}\to\tau_{21,\mathrm{rad}}^{\mathrm{mode}}$ and according to (69) β_{mode} approaches unity. Independent of the value of ℓ, suppression of all external modes and one polarization results in $1/\tau_{21,\mathrm{rad}}^{\mathrm{res}}=1/(2\tau_{21,\mathrm{rad}}^{\mathrm{tf\text{-}modes}})$, and when inserting the approximation of $\ell\to\infty$ from (72) and an equivalent of (55) into (74), one obtains $\beta_{\mathrm{mode}}\approx\lambda_e^2/(\pi\Delta\lambda_e\ell)$ for large ℓ, which is indicated by the black dashed line in Fig. 4, bottom row.

The spontaneous-emission rate of photons coupled per unit time interval into a single resonator mode and polarization is then given by

$$\begin{aligned} R_{\mathrm{sp}} &= \frac{\beta_{\mathrm{mode}}}{\tau_{21,\mathrm{rad}}^{\mathrm{res}}}N_2V_{\mathrm{mode}} = \frac{1}{\tau_{21,\mathrm{rad}}^{\mathrm{mode}}}N_2V_{\mathrm{mode}} \\ &= N_2V_{\mathrm{mode}}\int c\sigma_e(\nu)\tilde{M}_q(\nu)d\nu = N_2\int c\sigma_e(\nu)\tilde{\gamma}_q(\nu)d\nu \end{aligned} \tag{76}$$

R_{sp} is independent of β_{mode}, because it is triggered by the one vacuum photon φ_0 in this mode, which does not change in case the spontaneous-emission rate into other modes is manipulated. If the emission cross section is spectrally Lorentzian-shaped according to (53) and positioned at $\nu_e=\nu_q$, then inserting (53) and (22) into (76) and executing the integral leads to

$$R_{sp} = cN_2\sigma_e(\nu_e)\frac{\Delta\nu_e}{\Delta\nu_q+\Delta\nu_e}. \tag{77}$$

If the effective emission cross section $\sigma_e(\nu)$ varies insignificantly over the Lorentzian profile $\tilde{\gamma}_q(\nu)$ of the resonator mode, $\Delta\nu_e\gg\Delta\nu_q$, the spontaneous-emission rate of (76) and also that of (77) for the specific case of $\nu_e=\nu_q$ can be

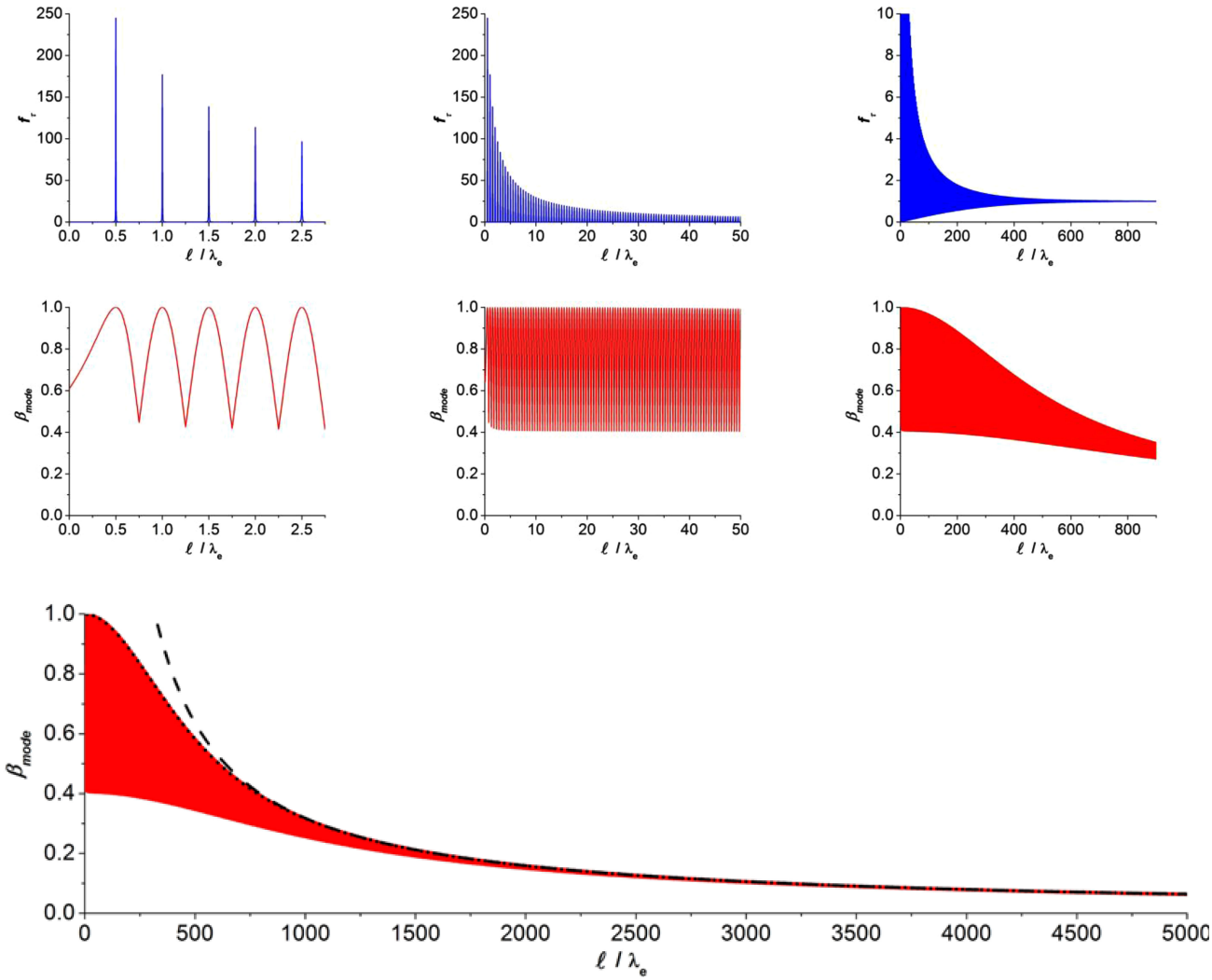

Fig. 4. Variation of spontaneous emission into the longitudinal, transverse-fundamental resonator modes, restricted to a single polarization, as a function of resonator length ℓ, normalized to the emission-peak wavelength λ_e, in a laser with $\lambda_e = 1$ μm, $\Delta\lambda_e = 1$ nm, $n_r = 1$, $T_{\rm out} = 0.01$ for all λ_q, and $L_{\rm RT} = 0$. Upper row: The enhancement factor f_τ of (73). Middle and bottom row: The fraction $\beta_{\rm mode}$ of (70), with (71) inserted. From left to right, different ranges of ℓ/λ_e are displayed. Bottom row: overview for a large range of ℓ values. Black dashed line: approximation for large ℓ as discussed in the text. Black dotted line: see the note added in proof.

approximated by

$$R_{\rm sp} = c\sigma_e(\nu_q)N_2. \tag{78}$$

Using the approximation of (78) in (76) yields (74).

B. Absorption and Amplification

In an absorbing, amplifying, or lasing resonator with a normalized spectral distribution function $\tilde{\gamma}_L(\nu)$ of the resonator mode centered at the frequency $\nu_{\rm L}$, the gain per unit length due to inversion between the population densities N_2 and N_1 in the upper and lower state, respectively, is accordingly given by

$$g = \int_0^\infty \Big[\sigma_e(\nu)N_2 - \sigma_a(\nu)N_1\Big]\tilde{\gamma}_L(\nu)d\nu. \tag{79}$$

Like for (78), if the effective emission and absorption cross sections $\sigma_e(\nu)$ and $\sigma_a(\nu)$, respectively, vary insignificantly over the Lorentzian profile $\tilde{\gamma}_L(\nu)$ of the resonator mode, $\Delta\nu_e$ and $\Delta\nu_a > \Delta\nu_L$, the gain per unit length can be approximated by

$$g = \sigma_e(\nu_L)N_2 - \sigma_a(\nu_L)N_1. \tag{80}$$

In case the gain medium absorbs light, $g < 0$, or amplifies light, $g > 0$ (as long as the loss-rate constant $1/\tau_c$ is larger than the gain-rate constant cg), the photon decay time τ_c of (13) decreases due to the additional loss (increases due to the gain) according to

$$\frac{1}{\tau_L} = \frac{1}{\tau_c} - cg \tag{81}$$

and the linewidth $\Delta\nu_c$ of (16) increases (decreases) to

$$\Delta\nu_L = \frac{1}{2\pi\tau_L} = \frac{1}{2\pi}\left(\frac{1}{\tau_c} - cg\right) = \Delta\nu_c - \frac{cg}{2\pi}. \tag{82}$$

As we will show, (81) and (82) also apply to the case of a lasing resonator mode [1].

C. The Fraction β of Upper-State Decay Rate Into the Resonator Mode

The total decay rate of the population density N_2 from the upper state per unit time can be written as

$$R_2 = \frac{1}{\tau_{2,\mathrm{eff}}^{\mathrm{res}}} N_2 V_{\mathrm{mode}}. \tag{83}$$

$\tau_{2,\mathrm{eff}}^{\mathrm{res}}$ is the effective decay time of the upper state of the emitter placed inside the resonator. We neglect nonlinear processes, e.g., fractional luminescence quenching [20], [21] or energy-transfer upconversion [21], owing to which $\tau_{2,\mathrm{eff}}^{\mathrm{res}}$ may deviate from the intrinsic lifetime τ_2^{res} of the upper state of the emitter placed inside the resonator. Again, if some external modes are suppressed by the resonator or if resonant enhancement occurs, $\tau_{2,\mathrm{eff}}^{\mathrm{res}}$ and τ_2^{res} may differ from the values in free space. Hence, with $\tau_{21,\mathrm{nrad}}$ and $\tau_{2,\mathrm{other}}$ considering relaxation from the upper state nonradiatively to the lower state and to other lower-lying levels, e.g., the ground state in a four-level laser, respectively,

$$\frac{1}{\tau_{2,\mathrm{eff}}^{\mathrm{res}}} \approx \frac{1}{\tau_2^{\mathrm{res}}} = \frac{1}{\tau_{21,\mathrm{rad}}^{\mathrm{res}}} + \frac{1}{\tau_{21,\mathrm{nrad}}} + \frac{1}{\tau_{2,\mathrm{other}}}. \tag{84}$$

We define

$$\beta_{21,\mathrm{rad}} := \frac{1/\tau_{21,\mathrm{rad}}^{\mathrm{res}}}{1/\tau_{2,\mathrm{eff}}^{\mathrm{res}}} \leq 1 \tag{85}$$

as the branching ratio of radiative decay from upper to lower state to total decay from the upper state. With (69) and (51), i.e., assuming that the emission cross section varies insignificantly over the linewidth of the resonator mode, we obtain

$$\begin{aligned}\frac{1}{\tau_{2,\mathrm{eff}}^{\mathrm{res}}} &= \frac{1}{\beta_{21,\mathrm{rad}}} \frac{1}{\tau_{21,\mathrm{rad}}^{\mathrm{res}}} = \frac{1}{\beta_{21,\mathrm{rad}}} \frac{1}{\beta_{\mathrm{mode}}} \frac{1}{\tau_{21,\mathrm{rad}}^{\mathrm{mode}}} \\ &= \frac{1}{\beta_{21,\mathrm{rad}}} \frac{1}{\beta_{\mathrm{mode}}} \frac{\int c\sigma_e(\nu)\tilde{\gamma}_q(\nu)d\nu}{V_{\mathrm{mode}}} \\ &\overset{\Delta\nu_e \gg \Delta\nu_q}{\approx} \frac{1}{\beta_{21,\mathrm{rad}}} \frac{1}{\beta_{\mathrm{mode}}} \frac{c\sigma_e}{V_{\mathrm{mode}}}.\end{aligned} \tag{86}$$

Consequently,

$$\beta = \beta_{21,\mathrm{rad}}\beta_{\mathrm{mode}} = \frac{c\sigma_e\tau_{2,\mathrm{eff}}^{\mathrm{res}}}{V_{\mathrm{mode}}} = \frac{R_{\mathrm{sp}}}{R_2} \leq 1 \tag{87}$$

is the fraction of total decay from the upper state that is coupled as spontaneous emission into the lasing resonator mode. By inserting (87) into (78) the spontaneous-emission rate into the lasing resonator mode then takes the familiar form

$$R_{\mathrm{sp}} = \frac{\beta}{\tau_{2,\mathrm{eff}}^{\mathrm{res}}} N_2 V_{\mathrm{mode}}. \tag{88}$$

When the mode volume is reduced to the fundamental modal dimensions of (30) and (32), $V_{\mathrm{mode}} \rightarrow V_{\mathrm{M}}$, specifically $\ell = \ell_M$ or a reasonably small integer multiple of ℓ_{M}, the emission is restricted to one polarization, and spontaneous emission into any other modes is suppressed, then β_{mode} approaches unity. If the population density of the upper state solely decays via spontaneous emission on the transition from upper to lower state, i.e., $\tau_{2,\mathrm{eff}}^{\mathrm{res}}$ equals the radiative lifetime $\tau_{21,\mathrm{rad}}^{\mathrm{res}}$ of the upper state when the gain medium is placed inside the resonator [RX1], then $\beta_{21,\mathrm{rad}} = 1$. Under these two conditions

$$\begin{aligned}\beta = \frac{c\sigma_e\tau_{2,\mathrm{eff}}^{\mathrm{res}}}{V_{\mathrm{mode}}} &\overset{\substack{\beta_{21,\mathrm{rad}}=1 \\ \beta_{\mathrm{mode}}=1}}{=} \frac{c\sigma_e\tau_{21,\mathrm{rad}}^{\mathrm{res}}}{V_{\mathrm{M}}} = c\sigma_e\tau_{21,\mathrm{rad}}^{\mathrm{res}} \frac{4\pi}{\lambda_e^3} = 1 \\ &\Rightarrow \sigma_e\tau_{21,\mathrm{rad}}^{\mathrm{res}}(V_M) = \frac{\lambda_e^3}{4\pi c}.\end{aligned} \tag{89}$$

Inserting the largest possible σ_e, namely the natural emission cross section of (56), provides the minimum possible radiative lifetime,

$$\tau_{21,\mathrm{rad}}^{\mathrm{res}}(V_M) = \frac{\lambda_e}{2c} = \frac{1}{2\nu_e} \tag{90}$$

and comparison of (89) with (58) delivers the fundamental emission linewidth and its related Q-factor,

$$Q_e = \frac{\lambda_e}{\Delta\lambda_e} = \frac{\nu_e}{\Delta\nu_e} = \pi. \tag{91}$$

Combination of (90) and (91) then reproduces (55).

D. Spontaneous Emission—A Time-Consuming Process

Semi-classically, a single photon is a spatially extended electromagnetic wave. The concept of temporal coherence implies that emission of a photon by an atom in an excited state with a characteristic decay time τ occurs as emission of a wave packet during the time interval τ, c.f. Fig. 1. Specifically, rearranging (74) yields

$$c\tau_{21,\mathrm{rad}}^{\mathrm{mode}}\sigma_e = c\frac{\tau_{21,\mathrm{rad}}^{\mathrm{res}}}{\beta_{\mathrm{mode}}}\sigma_e = V_{\mathrm{mode}} = \ell\pi w_0^2, \tag{92}$$

whose comparison with (7) shows that the time $\tau_{21,\mathrm{rad}}^{\mathrm{mode}}$ required to spontaneously emit a photon into a resonator mode equals the time the wave has to travel to fill the mode of length $\ell = c\tau_{21,\mathrm{rad}}^{\mathrm{mode}}$, in case $\sigma_{\mathrm{e}} = \sigma_{\mathrm{e,max}} = \lambda_e^2/(2\pi) = \pi w_M^2 = \pi w_0^2$. If the light-matter interaction is weaker, $\sigma_{\mathrm{e}} < \pi w_0^2$, because either the resonator mode has a larger area than the fundamental modal area, or the emitter has a smaller cross section than the natural cross section, or both, then a multi-pass interaction is required and, thus, the emission process takes accordingly longer. Spontaneous emission into a resonator is only possible if the emitted wave interferes constructively with itself after each round-trip, necessitating that it is emitted at the center frequency ν_q of the resonator mode. One can argue that ν_q is imposed upon the spontaneously emitted photon by the vacuum photon that carries the spectral properties of its birth-giving mode. This picture is consistent with describing the Casimir effect [22] as a result of vacuum fluctuations [23].

During the emission process, the photon energy is still partially stored in the excited state of the emitting atom and partially already emitted into the resonator mode, which is quantum-mechanically a superposition between the excited state and the de-excited state plus the emitted photon. Likewise, during the process of photon decay out of the resonator the front part of the wave packet already leaks out of the resonator, while its rear part is still oscillating inside the resonator. These two processes, emission of a photon into, and its decay out of the resonator, overlap in time.

Similar considerations hold true for stimulated-emission processes. Quantum-mechanically, the coherent photon number $\varphi_{\rm coh}$ existing in the lasing mode of the resonator represents the expectation value of the Poissonian photon statistics [24], which can assume non-integer values, just like the semi-classical $\varphi_{\rm coh}$ we will use in our work to describe a cw laser [1]. The creation and annihilation operators act on this coherent state. It is sometimes incorrectly assumed that these processes occur instantaneously by emission of a point-like photon, which would result in an instantaneously changing number of photons in the coherent state.

VI. Spontaneous Emission Into a Coherently Occupied Mode

So far we have investigated spontaneous emission into an empty resonator mode. In a laser, the lasing resonator mode is usually filled with a large number of coherent photons. This leads to a coupling between the atomic system and the coherent field, resulting in a splitting of the combined energy states and a modification of the spontaneous-emission rate into the lasing resonator mode.

A. Coupled Resonators of Atomic System and Coherent Field

The vacuum Rabi frequency is defined by [25]

$$h\nu_{\rm Rabi} = \mu E_V . \tag{93}$$

Therein,

$$\mu = e \left\langle 2 \right| r \left| 1 \right\rangle \tag{94}$$

is the dipole-transition matrix element for the transition between the states 2 and 1, where *e* is the electron charge and *e r* is the dipole operator. Furthermore,

$$E_V = \sqrt{\frac{h\nu}{2\varepsilon_0 V_{\rm mode}}} \tag{95}$$

shows the zero-point vacuum-fluctuation electric field, where ε_0 is the dielectric constant in vacuum. Inserting (94), (95), and the quantum-mechanical expression for the Einstein coefficient A_{21} [26],

$$A_{21} = \frac{1}{\tau_{21,\rm rad}} = \frac{2}{3}\frac{e^2 (2\pi)^3 \nu^3}{h\varepsilon_0 c^3} \left| \left\langle 2 \right| r \left| 1 \right\rangle \right|^2 , \tag{96}$$

into (93) yields an expression for the vacuum Rabi frequency [27] of an optical transition at the unperturbed frequency ν,

$$\nu_{\rm Rabi} = \frac{c}{4\pi\nu}\sqrt{\frac{3c}{2\pi V_{\rm mode}\tau_{21,\rm rad}}}. \tag{97}$$

As was shown by Jaynes and Cummings [28], the two atomic energy levels involved in an emission process and an electromagnetic field consisting of a number $\varphi_{\rm coh}$ of coherent photons in resonance with the transition constitute a system of coupled resonators, which are referred to as dressed states [29]. In a laser, the upper and lower non-degenerate atomic energy levels $|\psi_2>$ and $|\psi_1>$, respectively, of the gain medium and the coherent photon state $|\varphi_{\rm coh}>$ form common states $|\psi_2, \varphi_{\rm coh}>$ and $|\psi_1, \varphi_{\rm coh}>$, which for a variable coherent photon number $\varphi_{\rm coh}$ correspond to an equidistant ladder of energy states. In resonance, i.e., for a separation of the two atomic energy levels that equals the photon energy $h\nu_L$, the two upper states $|\psi_2, \varphi_{\rm coh}>$ and $|\psi_1, \varphi_{\rm coh}+1>$ of total energy $(\varphi_{\rm coh}+1)h\nu_L$ are degenerate, as are the two lower states $|\psi_2, \varphi_{\rm coh}-1>$ and $|\psi_1, \varphi_{\rm coh}>$ of total energy $\varphi_{\rm coh}h\nu_L$, see the left-hand side of Fig. 5(a). Assuming that after a pump process the atomic system is excited, while $\varphi_{\rm coh}$ photons are in the resonator, the system is in one of the two degenerate upper states, namely $|\psi_2, \varphi_{\rm coh}>$. Spontaneous emission of a photon into free space then turns the system into a superposition of $|\psi_1, \varphi_{\rm coh}>$ and $|\psi_2, \varphi_{\rm coh}-1>$, i.e., the total energy is reduced by the energy of the emitted photon from $(\varphi_{\rm coh}+1)h\nu_L$ to $\varphi_{\rm coh}h\nu_L$, where the lost energy may have emerged from either the atomic excitation or the coherent photon field. Spontaneous or stimulated emission into the lasing resonator mode results in the same reduction of total energy, because during the time interval when in a cw laser a photon is coupled into the lasing resonator mode, simultaneously another photon is coupled out (see Section V-C). With increasing strength of coupling between the atomic system and the coherent photon field, the degeneracy of each ladder state is lifted and the former degenerate combined states $|\psi_2, \varphi_{\rm coh}>$ and $|\psi_1, \varphi_{\rm coh}+1>$ are split by an amount of [30]

$$\delta E_{\rm Rabi} = 2h\nu_{\rm Rabi}\sqrt{\varphi_{\rm coh}+1}. \tag{98}$$

In this manner, the dressed states $|\varphi_{\rm coh}, \pm>$ are formed, resulting in a doublet splitting of each combined degenerate energy level as indicated on the right-hand side of Fig. 5(a). In the special case of $\varphi_{\rm coh}=0$, only one lower state $|\psi_1, 0>$ exists and, therefore, no splitting occurs in the lower level.

In the case where $n_{\rm m}$ two-level systems are present in the resonator mode and couple to the coherent field, i.e., in a four-level laser, in which the population density of the lower laser level is $N_1 = 0$, the number of excited states amounts to $n_m = b_2 N_2 V_{\rm mode}$, whereas in a three-level laser the total number of states, $n_m = (b_2 N_2 + b_1 N_1)V_{\rm mode}$, is in resonance with the mode, the total splitting of the lower and upper lasing state, respectively, is increased according to the Tavis-Cummings model [31] to

$$\delta E_{\rm Rabi} = 2h\nu_{\rm Rabi}\sqrt{n_m}\sqrt{\varphi_{\rm coh}+1}. \tag{99}$$

The coherent atom-field interaction that induces the dressed states, however, occurs only in the strong-coupling limit [32], where the Rabi oscillation can take place without being perturbed by de-coherence which is caused by, firstly, photon decay out of the resonator that is quantitatively represented by the coherence time $\tau_L^{\rm coh}$ of emitted laser light and, secondly, the atomic-state de-coherence that is quantitatively represented by $\tau_{\rm atom}^{\rm coh}$ of (52). Therefore, two conditions need to be fulfilled in order to obtain dressed states and the resulting level splitting:

$$2\pi\sqrt{n_m}\nu_{\rm Rabi} > \frac{1}{\tau_L^{\rm coh}} = \pi\Delta\nu_L \quad \text{and}$$

$$2\pi\sqrt{n_m}\nu_{\rm Rabi} > \frac{1}{\tau_{\rm atom}^{\rm coh}} = \pi\Delta\nu_e. \tag{100}$$

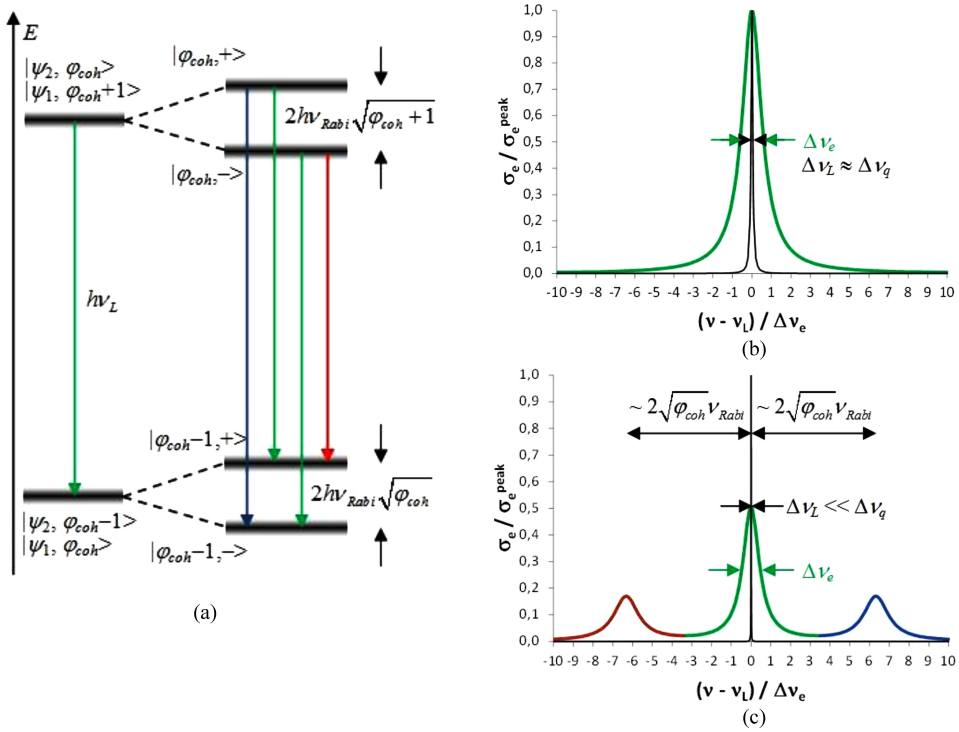

Fig. 5. Formation of a Mollow triplet for a single atom. (a) Energy levels and transitions. Spectral emission shapes (black curve) for the situations (b) with a weak and (c) with a strong coherent field (red curve) in the lasing resonator mode, under the assumption $\tau_{\mathrm{atom}}^{\mathrm{coh}} \gg \tau_{2,\mathrm{eff}}$ as in (103), resulting in $\Delta\nu_{e,sb} = 3/2\Delta\nu_e$. The laser linewidth $\Delta\nu_L$ is not to scale with the abscissa nor ordinate, but only indicative.

The typically long coherence time τ_L^{coh} of laser light significantly facilitates achieving the first condition. The second condition requires a long atomic coherence time $\tau_{\mathrm{atom}}^{\mathrm{coh}}$ of (52). Therefore, it can be reached more easily for lasers based on gain media which exhibit only natural linewidth broadening, i.e., de-phasing effects are negligible. It may be difficult to reach if only a single emitter is concerned, i.e., $n_m = 1$. However, if many laser-active states couple to the resonator field, $n_m \gg 1$, the second condition can be established thanks to the much larger effective Rabi frequency $\sqrt{n_m}\nu_{\mathrm{Rabi}}$ in (99).

B. Reduction of Spontaneous-Emission Rate and Mollow Triplet

With the normalized Lorentzian-shaped spectral mode profile of (22), the spontaneous-emission rate into a mode is given by (76). If the emission cross section is spectrally Lorentzian-shaped according to (53), with a peak value of $\sigma_e^{\mathrm{peak}} = \sigma_{\mathrm{e}}(\nu_{\mathrm{e}})$, the spontaneous-emission rate of (77) obtains. In the presence of a coherent field, the energetic splitting of (99) results in a division of the single spontaneous-emission line into four lines or, in the special case of $\varphi_{\mathrm{coh}} = 0$, a doublet spectrum and, consequently, a modification of the spontaneous-emission rate into the lasing resonator mode. Assuming that the original spontaneous-emission line is centered at the laser frequency ν_L, see Fig. 5(b), the four lines resulting from the interaction appear at frequencies

$$\begin{aligned}\nu_{p=1,\ldots,4} &= \nu_L + \delta\nu_{p=1,\ldots,4} \\ &= \nu_L \pm \left(\sqrt{\varphi_{\mathrm{coh}}+1} \pm \sqrt{\varphi_{\mathrm{coh}}}\right)\sqrt{n_m}\nu_{\mathrm{Rabi}}.\end{aligned} \tag{101}$$

With increasing number $\varphi_{\mathrm{coh}} \gg 1$ of coherent photons in the lasing mode and polarization of the resonator, resulting in a Rabi shift of $\delta\nu_{1,4} \gg \Delta\nu_e$, the spontaneous-emission spectrum under purely natural linewidth broadening evolves into the Mollow triplet [33], see Fig. 5(c), where one-half of the spontaneous emission ($p = 2$ and $p = 3$) overlaps almost perfectly at the central frequency ν_L, because in (101) $\sqrt{\varphi_{\mathrm{coh}}+1} - \sqrt{\varphi_{\mathrm{coh}}} \to 0$ for large φ_{coh}, whereas the other two peaks (the sidebands corresponding to $p = 1$ and $p = 4$) are spectrally further and further separated until they exhibit almost no spectral overlap with the lasing mode and, therefore, no contribution to spontaneous emission into this mode. The central line exhibits the original linewidth and the area ratio between the satellite peaks and the central peak is 1:2. Occurrence of the Mollow triplet has been experimentally verified [34].

From (41) it follows that, as long as the emission spectrum is narrow compared to its central frequency, $\Delta\nu_e \ll \nu_e$, the emission cross section has the same mathematical shape as the luminescence intensity. Therefore, Mollow's original derivation of the incoherent part of the luminescence intensity distribution,

cumulating in equation (4.33) of Ref. [33], can be used to describe the emission cross section in the presence of a strong coherent field. Thus, the formally Lorentzian-shaped emission cross section of (53) changes to the same three-peak structure and can be expressed as

$$\sigma_e^{\rm coh}(\nu) = \frac{1}{2}\sigma_e^{\rm peak}\frac{\Delta\nu_e^2}{4(\nu-\nu_e)^2+\Delta\nu_e^2} + \frac{1}{4}\frac{\Delta\nu_e}{\Delta\nu_{e,sb}}\sigma_e^{\rm peak}\frac{\Delta\nu_{e,sb}^2}{4\left(\nu-\nu_e-2\nu_{\rm Rabi}\sqrt{\varphi_{\rm coh}n_m}\right)^2+\Delta\nu_{e,sb}^2} + \frac{1}{4}\frac{\Delta\nu_e}{\Delta\nu_{e,sb}}\sigma_e^{\rm peak}\frac{\Delta\nu_{e,sb}^2}{4\left(\nu-\nu_e+2\nu_{\rm Rabi}\sqrt{\varphi_{\rm coh}n_m}\right)^2+\Delta\nu_{e,sb}^2}. \tag{102}$$

The emission bandwidth $\Delta\nu_{e,\rm sb}$ of the sidebands depends in a complex way on the strength of the atom-field coupling itself and the amount of de-coherence of the atomic system with coherence time $\tau_{\rm atom}^{\rm coh}$ compared to the decay-induced decoherence with upper-state effective luminescence decay time $\tau_{2,\rm eff}$. In some limiting cases we find

$$\Delta\nu_{e,sb} = \begin{cases} \Delta\nu_e & \text{for } \varphi_{\rm coh}\to 0 \\ \frac{3}{2}\Delta\nu_e & \text{for } \varphi_{\rm coh}\to\infty \text{ and } \tau_{\rm atom}^{\rm coh} >> \tau_{2,\rm eff} \\ \Delta\nu_e & \text{for } \varphi_{\rm coh}\to\infty \text{ and } \tau_{\rm atom}^{\rm coh} = 2\tau_{2,\rm eff} \\ \frac{1}{2}\Delta\nu_e & \text{for } \varphi_{\rm coh}\to\infty \text{ and } \tau_{\rm atom}^{\rm coh} << \tau_{2,\rm eff}. \end{cases} \tag{103}$$

In the case depicted in Fig. 5(c), the two satellite peaks have three-half the original linewidth, while the peak ratio is 1:3 [33].

Consequently, for $\delta\nu_{1,4} \gg \Delta\nu_e$, with (76) the effective spontaneous-emission rate into the lasing mode, with its Lorentzian-shaped mode profile $\tilde{\gamma}_L(\nu)$ and linewidth $\Delta\nu_L$, and polarization of the resonator becomes

$$\begin{aligned} R_{\rm sp,eff} &:= cN_2\int\sigma_e^{\rm coh}(\nu)\tilde{\gamma}_L\,d\nu \\ &= \frac{1}{2}cN_2\sigma_e^{\rm peak} \\ &\times\left[\frac{\Delta\nu_e}{\Delta\nu_L+\Delta\nu_e}+\frac{\Delta\nu_e(\Delta\nu_L+\Delta\nu_{e,sb})}{16\nu_{\rm Rabi}^2\varphi_{\rm coh}n_m+(\Delta\nu_L+\Delta\nu_{e,sb})^2}\right]. \end{aligned} \tag{104}$$

The ratio of the effective spontaneous-emission rate of (104) and the unperturbed spontaneous-emission rate of (76), in this case into a lasing resonator mode with a Lorentzian-shaped mode profile $\tilde{\gamma}_q(\nu) = \tilde{\gamma}_L(\nu)$ and linewidth $\Delta\nu_q = \Delta\nu_L$, provides the effective spontaneous-emission fraction,

$$\rho := \frac{R_{\rm sp,eff}}{R_{\rm sp}} = \frac{cN_2\int\sigma_e^{\rm coh}(\nu)\tilde{\gamma}_L\,d\nu}{cN_2\int\sigma_e(\nu)\tilde{\gamma}_L\,d\nu}. \tag{105}$$

In case the emission line is of Lorentzian shape, inserting (104) and (77), again with $\Delta\nu_q = \Delta\nu_L$, into (105) yields

$$\rho = \frac{1}{2}+\frac{1}{2}\frac{(\Delta\nu_L+\Delta\nu_e)(\Delta\nu_L+\Delta\nu_{e,\rm sb})}{16\nu_{\rm Rabi}^2\varphi_{\rm coh}n_m+(\Delta\nu_L+\Delta\nu_{e,\rm sb})^2} \overset{\varphi_{\rm coh}\to\infty}{\approx} \frac{1}{2}. \tag{106}$$

Since the Rabi shifts $\delta\nu_p$ in (101) depend on the coherent photon number $\varphi_{\rm coh}$ in the lasing mode, ρ changes from unity at low $\varphi_{\rm coh}$, where the peaks of all four emission lines are spectrally positioned within the laser linewidth and exhibit the same bandwidth $\Delta\nu_e$, down to the value of ½ at large $\varphi_{\rm coh}$, thereby reducing the spontaneous-emission rate into the lasing resonator mode at large $\varphi_{\rm coh}$ to ½ its value into an empty resonator mode.

Whenever a significant atom-field interaction is present, i.e., $\rho < 1$, the fractions $\beta_{\rm mode}$ and β are affected and must be modified.

VII. Conclusion

In this paper, we have revisited the physics underlying the process of spontaneous emission into a resonator mode. We have verified that the spontaneous-emission rate into a resonator mode is equal to the stimulated-emission rate driven by the one vacuum photon that is present inside this mode. This rate is independent of spontaneous emission into other modes. By considering the fundamental modal dimensions, we have derived novel physical expressions for the fractions of spontaneous emission and total decay from the upper laser level into this mode, which show that these fractions necessarily depend on the specific resonator configuration and resulting spontaneous emission into all other available modes. We have also investigated the coupling of the atomic system with the coherent field inside a lasing resonator mode and derived an expression for the effective emission cross section and resulting fraction of the spontaneous-emission rate into a lasing resonator mode under the influence of this interaction.

In our subsequent work [1], we will exploit this physical foundation for establishing a refined and more complete description of the cw laser.

Note added in proof: In the situation underlying (70), if the resonator length ℓ is tuned, such that one longitudinal resonator mode with index m spectrally overlaps with the Lorentzian-shaped emission line, $\nu_m = \nu_e$, and assuming that the resonator losses do not vary significantly over the spectral range of the emission line, $\Delta\nu_q \approx \Delta\nu_m = \Delta\nu_c$ for all modes with index q that exhibit a relevant overlap with the emission line, then by inserting the result of (71) into both the numerator and denominator of (70) one obtains

$$\beta_{\rm mode} = \frac{1}{\sum_{q=0}^{\infty}\frac{(\Delta\nu_c+\Delta\nu_e)^2}{4(\nu_e-\nu_q)^2+(\Delta\nu_c+\Delta\nu_e)^2}} \tag{107}$$

This is the dotted black line in Fig. 4, bottom row.

References

[1] M. Eichhorn and M. Pollnau, "The theory of continuous-wave lasers in the spot light of spontaneous emission" to be published.

[2] A. Einstein, "Zur Quantentheorie der Strahlung," *Phys. Z.*, vol. 18, no. 6, pp. 121–128, 1917.

[3] W. Heisenberg, "Über den anschaulichen Inhalt der quantentheoretischen Kinematik und Mechanik," *Z. Phys.*, vol. 43, no. 3–4, pp. 172–198, 1927.

[4] H. P. Robertson, "The uncertainty principle," *Phys. Rev.*, vol. 34, no. 1, pp. 163–164, 1929.

[5] B. A. Lengyel, *Lasers*, 2nd ed. New York, NY, USA: Wiley, 1971, p. 81 ff.

[6] M. Planck, "Ueber das Gesetz der Energieverteilung im Normalspectrum," *Ann. Phys.*, vol. 309, no. 3, pp. 553–563, 1901.

[7] B. E. A. Saleh and M. C. Teich, *Fundamentals of Photonics*, 2nd ed. Hoboken, NJ, USA: Wiley-Interscience, 2007, pp. 408–409.
[8] K. S. Johnson, *Transmission Circuits For Telephonic Communication*, 5th ed., D. Van Nostrand, Eds. New York, NY, USA: Western ElectricIn, 1931, ch. XV, pp. 174–179.
[9] H. H. Hansen, "A type of electrical resonator," *J. Appl. Phys.*, vol. 9, no. 10, pp. 654–663, 1938.
[10] C. Fabry and A. Pérot, "Théorie et applications d'une nouvelle méthode de spectroscopie interférentielle," *Ann. de Chim. et de Phys.*, vol. 16, no. 7, pp. 115–144, 1899.
[11] G. B. Airy, "On the intensity of light in the neighbourhood of a caustic," *Trans. Camb. Phil. Soc.*, vol. 6, no. 3, pp. 379–402, 1838.
[12] O. Svelto, *Principles of Lasers*, 5th ed. New York, NY, USA: Springer, 2010, pp. 142–146.
[13] E. M. Purcell, "Spontaneous emission probabilities at radio frequencies," *Phys. Rev.*, vol. 69, no. 11/12, p. 681, 1946.
[14] E. Affolter and F. K. Kneubühl, "Far-infrared distributed feedback gas laser," *IEEE J. Quantum Electron.*, vol. QE-17, no. 6, pp. 1115–1122, Jun. 1981.
[15] P. Schwaller, H. Steffen, J. F. Moser, and F. K. Kneubühl, "Interferometry of resonator modes in submillimeter wave lasers," *Appl. Opt.*, vol. 6, no. 5, pp. 827–829, 1967.
[16] D. Geskus, S. Aravazhi, S. M. García-Blanco, and M. Pollnau, "Giant optical gain in a rare-earth-ion-doped microstructure," *Adv. Mater.*, vol. 24, no. 10, pp. OP19–OP22, 2012.
[17] N. V. Kuleshov, A. A. Lagatsky, V. G. Shcherbitsky, V. P. Mikhailov, E. Heumann, T. Jensen, A. Diening, and G. Huber, "CW laser performance of Yb and Er, Yb doped tungstates," *Appl. Phys. B*, vol. 64, no. 4, pp. 409–413, 1997.
[18] A. A. Lagatsky, N. V. Kuleshov, and V. P. Mikhailov, "Diode-pumped CW lasing of Yb:KYW and Yb:KGW," *Opt. Commun.*, vol. 165, no. 1–3, pp. 71–75, 1999.
[19] S. Aravazhi, D. Geskus, K. van Dalfsen, S. A. Vázquez-Córdova, C. Grivas, U. Griebner, S. M. García-Blanco, and M. Pollnau, "Engineering lattice matching, doping level, and optical properties of $KY(WO_4)_2$:Gd,Lu,Yb layers for a cladding-side-pumped channel waveguide laser," *Appl. Phys. B*, vol. 111, no. 3, pp. 433–446, 2013.
[20] L. Agazzi, E. H. Bernhardi, K. Wörhoff, and M. Pollnau, "Impact of luminescence quenching on relaxation-oscillation frequency in solid-state lasers," *Appl. Phys. Lett.*, vol. 100, no. 1, article 011109, 2012.
[21] L. Agazzi, K. Wörhoff, and M. Pollnau, "Energy-transfer-upconversion models, their applicability and breakdown in the presence of spectroscopically distinct ion classes: A case study in amorphous $Al_2O_3:Er^{3+}$," *J. Phys. Chem. C*, vol. 117, no. 13, pp. 6759–6776, 2013.
[22] H. B. G. Casimir, "On the attraction between two perfectly conducting plates," in *Proc. Kon. Ned. Akad. Wetensch.*, 1948, vol. B51, pp. 793–796.
[23] P. W. Milonni, *The Quantum Vacuum: An Introduction to Quantum Electrodynamics*. San Diego, CA, USA: Academic, 1994.
[24] M. Sargent III, M. O. Scully, and W. E. Lamb, Jr., *Laser Physics*, 6th ed. Boulder, CO, USA: Westview Press, 1993, ch. 15, pp. 242–255.
[25] R. Loudon, *The Quantum Theory of Light*, Oxford, U.K.: Oxford Univ. Press, 2000, p. 172.
[26] F. Schwabl, *Quantenmechanik*, Berlin, Germany: Springer, 1988, p. 262.
[27] I. I. Rabi, "Space quantization in a gyrating magnetic field," *Phys. Rev.*, vol. 51, no. 8, pp. 652–654, 1937.
[28] E. T. Jaynes and F. W. Cummings, "Comparison of quantum and semiclassical radiation theories with application to the beam maser," *Proc. IEEE*, vol. 51, no. 1, pp. 89–109, Jan. 1963.
[29] C. Cohen-Tannoudji, J. Dupont-Roc, and G. Grynberg, *Processus D'interaction Entre Photons et Atomes*. Paris, Italy: InterEditions et Editions du CNRS, 1988.
[30] M. Sargent III, M. O. Scully, and W. E. Lamb, Jr., *Laser Physics*, 6th ed. Boulder, CO, USA: Westview Press, 1993, ch. 14, sec. 1–3, pp. 222–236.
[31] M. Tavis and F. W. Cummings, "Exact solution for an N-molecule-radiation-field Hamiltonian," *Phys. Rev.*, vol. 170, no. 2, pp. 379–384, 1968.
[32] H. J. Kimble, *Cavity Quantum Electrodynamics*. San Diego, CA, USA: Academic, 1994, vol. 2, pp. 203–266.
[33] B. R. Mollow, "Power spectrum of light scattered by two-level systems," *Phys. Rev.*, vol. 188, no. 5, pp. 1969–1975, 1969.
[34] A. Ulhaq, S. Weiler, C. Roy, S. M. Ulrich, M. Jetter, S. Hughes, and P. Michler, "Detuning-dependent mollow triplet of a coherently-driven single quantum dot," *Opt. Exp.*, vol. 21, no. 4, pp. 4382–4395, 2013.

Marc Eichhorn received the Diploma degree in physics from the University of Heidelberg, Heidelberg, Germany, in 2003, for his work on high-power CO_2 lasers and ultra-cold atoms and the Dr. rer. nat. degree from the University of Freiburg, Germany, in 2005, for his research on IR fiber lasers and chalcogenide lasers. In 2009, he performed his habilitation in experimental physics at the University of Hamburg, Hamburg, Germany, on quasi-three-level solid-state lasers. Since 2003, he has been with the French-German Research Institute of Saint-Louis (ISL), where he holds the position of head of Division III (Laser and electromagnetic technologies). His main research interests include high-power diode-pumped solid-state lasers, heat-capacity lasers, fiber lasers in the near- and mid-infrared, laser materials as well as mid-infrared nonlinear wavelength conversion and associated materials. He is a Member of the Optical Society of America and the German Physical Society.

Markus Pollnau received the M.Sc. degree from the University of Hamburg, Hamburg, Germany, in 1992, and the Ph.D. degree from the University of Bern, Bern, Switzerland, in 1996, both in physics.

After postdoctoral positions with the University of Southampton and the University of Bern, he was a Project and Research Group Leader with the Swiss Federal Institute of Technology, Lausanne, Switzerland. In 2004, he became a Full Professor and the Chair of the Integrated Optical MicroSystems Group, MESA+ Institute for Nanotechnology, University of Twente, Enschede, The Netherlands. In 2014, he moved to the Department of Materials and Nano Physics, KTH—Royal Institute of Technology, Stockholm, Sweden. He has contributed to more than 500 reviewed journal and international conference papers and eleven book chapters in the fields of crystal and thin-film growth, rare-earth-ion spectroscopy, solid-state and fiber lasers, and waveguide fabrication, devices, and applications.

Dr. Pollnau has held European, Swiss, and Dutch personal Fellowships and received numerous National and European Research Grants. In 2013, he received the ERC Advanced Grant "Optical Ultra-Sensor" of the European Research Council. He has been involved in the organization of major international conferences, e.g., as a Program and General Cochair of the Conference on Lasers and Electro-Optics (2006/2008) and the Conference on Lasers and Electro-Optics Europe (2009/2011), and served as a Topical Editor for the *Journal of the Optical Society of America B* and on the editorial board of the journal *Laser Physics Letters*. He was elected as a Fellow of the Optical Society of America in 2013 and a Fellow of the European Physical Society in 2014.